Gene duplication and rate variation in the evolution of non-photosynthetic pathways in plastids

Alissa M. Williams[1,2,*], Olivia G. Carter[1], Evan S. Forsythe[1], Hannah K. Mendoza[1], Daniel B. Sloan[1]

[1]Department of Biology, Colorado State University, Fort Collins, Colorado 80523

[2]Program in Cell and Molecular Biology, Colorado State University, Fort Collins, Colorado 80523

*corresponding author: Alissa.Williams@colostate.edu

Abstract:

While the chloroplast (plastid) is known for its role in photosynthesis, it is also involved in many other biosynthetic pathways essential for plant survival. As such, plastids contain an extensive suite of enzymes required for non-photosynthetic processes. The evolution of the associated genes has been especially dynamic in flowering plants (angiosperms), including examples of gene duplication and extensive rate variation. We examined the role of ongoing gene duplication in two key plastid enzymes, the acetyl-CoA carboxylase (ACCase) and the caseinolytic protease (Clp), responsible for fatty acid biosynthesis and protein turnover, respectively. In plants, there are two ACCase complexes—a homomeric version present in the cytosol and a heteromeric version present in the plastid. Duplications of the nuclear-encoded homomeric ACCase gene and retargeting to the plastid have been previously reported in multiple species. We find that these retargeted copies of the homomeric ACCase gene exhibit elevated rates of sequence evolution, consistent with neofunctionalization and/or relaxation of selection. The plastid Clp complex catalytic core is composed of nine paralogous proteins that arose via ancient gene duplication in the cyanobacterial/plastid lineage. We show that further gene duplication occurred more recently in the nuclear-encoded core subunits of this complex, yielding additional paralogs in many species of angiosperms. Moreover, in six of eight cases, subunits that have undergone recent duplication display increased rates of sequence evolution relative to those that have remained single copy. We also compared rate patterns between pairs of Clp core paralogs to gain insight into post-duplication evolutionary routes. These results show that gene duplication and rate variation continue to shape the plastid proteome.

Introduction:

The plastid is a dynamic proteomic environment in which key photosynthetic and non-photosynthetic biochemical reactions occur. Major non-photosynthetic functions of plastids include the reaction catalyzed by the acetyl-CoA carboxylase (ACCase) enzyme and protein degradation performed by the caseinolytic protease (Clp) complex (Caroca et al., 2021; Green, 2011; Konishi et al., 1996; Nishimura et al., 2017; Nishimura and van Wijk, 2015). Both of these functions are essential in plants and thus the genes involved are generally highly conserved; however, these genes have undergone rapid evolution in multiple angiosperm species (Barnard-Kubow et al., 2014; Erixon and Oxelman, 2008; Jansen et al., 2007; Park et al., 2017; Sloan et al., 2014, 2014; Wicke et al., 2011; Williams et al., 2019, 2015; Zhang et al., 2014). While many hypotheses about these patterns of accelerated evolution have been posited, the underlying evolutionary mechanisms, causes, and consequences remain largely unknown.

The ACCase enzyme catalyzes the first committed step of fatty acid biosynthesis, the carboxylation of acetyl-CoA to malonyl-CoA (Salie and Thelen, 2016; Sasaki and Nagano, 2004). This step requires four different enzyme domains—one biotin carboxylase, one biotin carboxyl carrier, and two (α and β) carboxyltransferases (Salie and Thelen, 2016; Sasaki and Nagano, 2004; Schulte et al., 1997). In plants, there are two forms of the ACCase enzyme. The homomeric version, present in the cytosol, is encoded by a single nuclear gene (Konishi et al., 1996; Konishi and Sasaki, 1994). The heteromeric version, present in the plastid, is encoded by five genes in *Arabidopsis thaliana*; each functional domain is represented by a single gene except for the biotin carboxyl carrier domain, which is encoded by two genes (Konishi et al., 1996; Konishi and Sasaki, 1994; Salie and Thelen, 2016). Four of these genes are in the nuclear genome while the fifth (*accD*) is in the plastid genome (Caroca et al., 2021; Sasaki and Nagano, 2004). In a few angiosperm lineages, including the Brassicaceae, Caryophyllaceae, Geraniaceae, and Poaceae, there have been duplications of the homomeric ACCase gene with subsequent retargeting of one copy to the plastid (Babiychuk et al., 2011; Konishi and Sasaki, 1994; Park et al., 2017; Parker et al., 2014; Rockenbach et al., 2016; Schulte et al., 1997).

The Clp complex is one of the most abundant stromal proteases and degrades a variety of targets (Apitz et al., 2016; Bouchnak and van Wijk, 2021; Majeran et al., 2000; Montandon et al., 2019; Nishimura et al., 2017; Nishimura and van Wijk, 2015; Welsch et al., 2018). This complex consists of many types of subunits. Adapters bind proteins targeted for degradation and deliver them to chaperones, which use ATP to unfold the targeted proteins into the proteolytic core of the complex (Nishimura and van Wijk, 2015). The core consists of 14 subunits that are encoded by nine different paralogous genes (Olinares et al., 2011a; Peltier et al., 2004; Sjögren et al., 2006; Stanne et al., 2007). Eight of these genes reside in the nuclear genome (*CLPP3-6, CLPR1-4*), while the ninth is encoded in the plastid genome (*clpP1*) (Nishimura et al., 2017; Olinares et al., 2011b). The ClpP subunits contain a catalytically active Ser-His-Asp triad, whereas the ClpR subunits do not (Nishimura and van Wijk, 2015; Porankiewicz et al., 1999). These nine paralogs are the results of gene duplications throughout cyanobacterial and plastid evolution and are shared by all land plants (Olinares et al., 2011a). Ongoing gene duplication of individual subunits has been noted in a handful of angiosperm lineages (Rockenbach et al., 2016; Williams et al., 2021, 2019).

Thus, the evolutionary trajectory of both of these essential plastid pathways is characterized by gene duplication at both ancient and recent timescales. Gene duplication is common in land plants, in part due to the frequency with which whole genome duplication (polyploidization) occurs in this lineage (Clark and Donoghue, 2018; De Bodt et al., 2005; del Pozo and Ramirez-Parra, 2015; Flagel and Wendel, 2009; Panchy et al., 2016; Wendel et al., 2018). Nearly all species of land plants have polyploidization events in their evolutionary histories (Clark and Donoghue, 2018; Leebens-Mack et al., 2019; Panchy et al., 2016). Angiosperms in particular seem to have a propensity for whole genome duplication; the entire clade shares an ancient polyploidization event and many lineages have undergone subsequent rounds of whole genome duplication (Clark and Donoghue, 2018; Panchy et al., 2016; Renny-Byfield and Wendel, 2014; Soltis et al., 2009). While every gene is initially affected by whole genome duplication, only 10-30% of those duplicates are maintained in the genome longer-term (Hahn, 2009; Maere et al., 2005; Paterson et al., 2006). Though polyploidy is likely a main contributor to gene duplication in plants, other forms of gene duplication are also prevalent (Flagel and Wendel, 2009). For instance, tandem duplication has been shown to be common in both *Arabidopsis thaliana* and

Oryza sativa, where tandemly arrayed gene clusters make up 15-20% of genic content. Additionally, multiple studies have shown that transposon-mediated gene duplication is prevalent in plants (Flagel and Wendel, 2009; Freeling et al., 2008; Rizzon et al., 2006; Wang et al., 2006).

Gene duplication is an important evolutionary process and is thought to be a major source of evolutionary novelty (Hahn, 2009; Ohno, 1970; Taylor and Raes, 2004; Zhang, 2003). The most common evolutionary fate of paralogs is retention of one copy and pseudogenization and loss of the other copy (Lynch and Conery, 2000; Zhang, 2003; Zhang et al., 2003). However, several evolutionary mechanisms have been described in which retention of both gene duplicates is favored. The increased gene-dosage advantage model describes a scenario in which increased amount of gene product produced by the two identical gene copies is beneficial and thus both copies retain ancestral function (Hahn, 2009; Ohno, 1970; Pegueroles et al., 2013; Zhang, 2003). The neofunctionalization model posits that one paralog acquires new functions while the other retains ancestral functionality (Hahn, 2009; Ohno, 1970; Pegueroles et al., 2013; Zhang, 2003). In the subfunctionalization model, an ancestral function is split between the two duplicates (Hahn, 2009; Ohno, 1970; Pegueroles et al., 2013; Zhang, 2003), in some cases creating the possibility for each paralog to optimize a subset of the ancestral function in a process known as escape from adaptive conflict (Des Marais and Rausher, 2008; Huang et al., 2015; Sikosek et al., 2012).

To distinguish between these evolutionary fates, many studies have employed evolutionary rate comparisons (Hahn, 2009; Pegueroles et al., 2013). These comparisons involve both paralogs as well as their common ancestor (Pegueroles et al., 2013). Under both the gene-dosage advantage and subfunctionalization models, gene duplicates are expected to evolve at approximately the same rate as each other (Pegueroles et al., 2013). The difference in evolutionary rates predicted by these two models is found in comparisons to the common ancestor; with a gene-dosage advantage, the expectation is that the paralogs will evolve at the same rate as the common ancestor, while with subfunctionalization, the expectation is that the paralogs will evolve at an increased rate relative to the common ancestor (though this assumption has been challenged) (Force et al., 1999; Hahn, 2009; He and Zhang, 2005; Lynch and Force, 2000; Pegueroles et al.,

2013; Zhang, 2003). By contrast, under the neofunctionalization model, asymmetry between evolutionary rates of paralogs is expected, where one paralog retains the ancestral evolutionary rate while the other experiences rate acceleration after being freed from selective constraints (Hahn, 2009; Pegueroles et al., 2013; Zhang, 2003). The proportion of paralogs with asymmetric rates of evolution has been estimated at anywhere from 5% to 65% in a variety of studies (Conant and Wagner, 2003; Dermitzakis and Clark, 2001; Kondrashov et al., 2002; Panchin et al., 2010; Pegueroles et al., 2013; Van de Peer et al., 2001). This wide range of estimates is likely due to differences in study systems, definitions and identifications of paralogs, gene types, and time since duplication. Despite the varying estimates of evolutionary rate asymmetry, it is clear that paralogs evolve under a mixture of evolutionary regimes.

Here, we characterize recent gene duplication events and subsequent changes in evolutionary rate in ACCase and Clp core subunits. We show that ACCase genes exhibit patterns of duplication, retargeting, and accelerated protein evolution consistent with neofunctionalization and/or relaxed selection. Additionally, we examine duplications of nuclear-encoded plastid Clp core subunits and demonstrate that duplication leads to significant changes in the rate of evolution in most cases but that patterns differ across Clp subunits, meaning multiple post-duplication evolutionary routes are represented across pairs of paralogs. This work provides additional insights into the interplay between gene duplication and evolutionary rate in the molecular evolution of plastid proteins.

Materials and Methods:

Compilation and curation of *ACC* nucleotide sequences

Previous work identified duplications of the homomeric ACCase gene *ACC* and subsequent retargeting of one copy to the plastid in the angiosperm families Poaceae (Konishi and Sasaki, 1994; Park et al., 2017; Rockenbach et al., 2016), Brassicaceae (Babiychuk et al., 2011; Park et al., 2017; Parker et al., 2014; Schulte et al., 1997), Caryophyllaceae (Rockenbach et al., 2016), and Geraniaceae (Park et al., 2017). *ACC* genes were obtained for multiple species in each of these families. All cytosol-targeted *ACC* genes were designated *ACC1* while all plastid-targeted

ACC genes were designated *ACC2* per established conventions (Babiychuk et al., 2011; Sasaki and Nagano, 2004); thus, sharing the same identifier does not necessarily indicate orthology because of the multiple independent origins of plastid-targeted *ACC2* genes. *Amborella trichopoda*, which has a single *ACC* gene that we designated *ACC1*, was used as an outgroup.

Trimmed *ACC1* and *ACC2* coding sequences (CDSs) were obtained from Rockenbach et al. (2016) for *Amborella trichopoda, Arabidopsis thaliana, Agrostemma githago*, *Silene noctiflora*, *Silene paradoxa,* and *Triticum aestivum*. The trimming in Rockenbach et al (2016) was codon-guided and included removal of the target peptide. *ACC1* and *ACC2* CDSs from the following species were compiled using gene identifiers from Table S4 in Park et al. (2017): Geraniaceae: *California macrophylla, Erodium texanum, Geranium incanum, Geranium maderense, Geranium phaeum, Monsonia emarginata, Pelargonium cotyledonis*; Brassicaceae: *Capsella rubella*; Poaceae: *Oryza sativa*, *Sorghum bicolor*. Duplications of *ACC* were additionally identified in two Poaceae species—*Aegilops tauschii* and *Zea mays*—by performing BLAST searches against these organisms on NCBI and Phytozome v13, respectively (Camacho et al., 2009; Goodstein et al., 2012).

All *ACC1* and *ACC2* sequences were included in a single file and aligned using the MAFFT *einsi* option (Katoh and Standley, 2013) in codon space using the *align_fasta_with_mafft_codon* subroutine in the sloan.pm Perl module (https://github.com/dbsloan/perl_modules). 5′ trimming was conducted according to the trimming performed in Rockenbach et al. (2016). Additional trimming of poorly aligned regions was performed manually in a codon-based manner.

Compilation and curation of Clp core subunit amino acid and nucleotide sequences

To identify Clp core subunit amino acid sequences, a custom Python script (https://github.com/alissawilliams/Gene_duplication_ACCase_Clp/scripts /local_blast5.py) was used to reciprocally blast (blastp v2.2.29) *Arabidopsis thaliana* amino acid sequences against predicted protein sequences from each of 22 other angiosperm species in the dataset. These 22 species were the same set used in Williams et al. (2019) with the exclusion of *Silene latifolia* and *Silene noctiflora*, since Clp core subunit duplications have been previously studied in *Sileneae*

(Rockenbach et al., 2016; Williams et al., 2021, 2019). This sampling was chosen to represent both the diversity of angiosperms and the range of rate variation in Clp complex evolution (Williams et al., 2019; see Table S3).

Compiled amino acid sequences for each subunit were aligned using the *einsi* option in MAFFT v7.222 (Katoh and Standley, 2013) and trimmed using GBLOCKS v0.91b (Castresana, 2000) with parameter *-b1* set to the default value of *-b2* and parameter *-b5* set to *h*. All alignments were examined manually to confirm homology. Sequences were also screened to prevent inclusion of multiple splice variants from a single gene. In cases where genomic data were used, only one transcript per gene was used. In cases where transcriptomic data were used, sequences were eliminated when alternative splicing was obvious (i.e. inclusion of an intron where the other sequence had a gap or variation only in one short piece of the transcript at either end). Catalytic site status and length were determined using the amino acid sequence data.

Nucleotide sequences for each identified Clp core subunit protein sequence were compiled from the corresponding CDS or transcript sequence file. For non-CDS sequences, ORFfinder (Wheeler et al., 2003) was used to identify the coding sequence. Compiled CDS sequences for each subunit were aligned with the MAFFT *einsi* option (Katoh and Standley, 2013) in codon space as above. 5′ and 3′ end trimming was performed manually in a codon-based manner.

Generating constraint trees for the *ACC* and Clp subunit alignments for use in PAML

A constraint tree stipulates a fixed topology (branching order) that is used by a phylogenetic program (in this case, PAML) when calculating branch lengths. To generate a constraint tree for the *ACC* alignment, RAxML v8.2.12 (Stamatakis, 2014) was used on the trimmed nucleotide alignment with parameters *-m = GTRGAMMA, -p = 12345, -f = a, -x = 12345,* and *-# = 100*. The resultant topology confirmed that there were independent *ACC* duplications at the base of each family (Park et al., 2017; Rockenbach et al., 2016).

To construct constraint trees for Clp core subunits, each trimmed amino acid alignment was analyzed with ProtTest v3.4.2 (Darriba et al., 2011) to choose a model of sequence evolution.

The top model based on the Bayesian Information Criterion was chosen for use in PhyML v3.3 (Guindon et al., 2010), which was run with 1000 bootstrap replicates and 100 random starts. The resultant phylogenetic trees were used to determine whether duplication events were lineage-specific or shared among species in the dataset. In almost all cases, paralogs from a single species were sister to one another in the trees, indicating lineage-specific duplications. There were a few cases in which paralogs from a single species were not sister to one another. However, given low bootstrap support and the difficulty of resolving species relationships using a single gene with highly variable rates of evolution, we proceeded under the assumption that these duplications were lineage-specific as well. Thus, the constraint trees for each individual Clp core subunit were constructed using the known species tree (The Angiosperm Phylogeny Group et al., 2016), with duplications encoded as species-specific (mapped to terminal branches of the species tree).

Running PAML for ACCase and Clp core subunit genes

For each alignment, PAML v4.9j (Yang, 2007) was used to infer d_N/d_S values for all branches using the free ratios model (model = 1) and parameters *CodonFreq = 2* and *cleandata = 0*. Additionally, *model = 0* and *model = 2* runs were conducted for all alignments, again using *CodonFreq = 2* and *cleandata = 0*. The *model = 0* runs forced all branches to have the same d_N/d_S ratio, while the *model = 2* runs allowed different d_N/d_S values for specified groups of branches.

For the *ACC* alignment, one *model = 2* run was conducted with plastid-targeted branches as the foreground. The resultant tree had one d_N/d_S value for plastid-targeted (*ACC2*) branches and a second d_N/d_S value for cytosol-targeted (*ACC1*) branches (including all internal pre-duplication branches). This output was compared with the *model = 0* run to determine whether allowing two d_N/d_S ratios (one for each of those groups) was a better fit to the data than allowing just a single d_N/d_S value. For the Clp subunit alignments, *model = 2* was used twice. In the first run, all terminal branches (and in the case of two subunits, internal post-duplication branches) were designated as the foreground. In the second run, there were three classes of branches, where all branches were categorized the same as in the first run except that post-duplication branches

(internal or terminal) were placed in a third category. The three-partition and two-partition models were compared to determine whether allowing an additional d_N/d_S ratio for post-duplication branches was a better fit to the data than just separating terminal from internal branches. The models were compared using likelihood ratio tests.

For the *ACC* alignment, a branch-site test (Yang, 2007; Yang and Nielsen, 2002) was also conducted to test for evidence of positive selection on branches for plastid-targeted genes, which were set as the foreground branches for this analysis. A null model and an alternative model both used the parameters *model = 2, NSsites = 2, CodonFreq = 2*, and *cleandata = 0*. The alternative model otherwise used all default values, while the null model additionally used *fix_omega = 1* and *omega = 1*. The models were compared using a likelihood ratio test.

Running HyPhy for *ACC*

In addition to running a PAML branch-site test on the *ACC* alignment (Yang, 2007; Yang and Nielsen, 2002), tests for positive and relaxed selection were implemented in HyPhy v2.5.32 (Kosakovsky Pond et al., 2020). Positive selection was tested for using the aBSREL and BUSTED methods (Murrell et al., 2015; Smith et al., 2015). The RELAX method was used to test for relaxed vs. intensified selection (Wertheim et al., 2015). As with the PAML runs, the constraint tree used for HyPhy methods had the branches separated into two categories (*ACC1* and *ACC2*).

Comparisons between *ACC1* and *ACC2* genes

To compare d_N and d_S between cytosolic-targeted and plastid-targeted *ACC* genes (*ACC1* and *ACC2*, respectively), a mean root-to-tip distance was calculated for each family in the tree. The base of each duplication event was used as the root for each family. For both d_N and d_S, the four mean distances for *ACC1* were compared to those of *ACC2* using a paired t-test in R. Because of the *a priori* prediction that retargeting to the plastid would be associated with accelerated protein sequence evolution, a one-sided test (*ACC2 > ACC1*) was used for d_N, while a two-sided test was used for d_S.

Fisher's exact test on Clp subunit paralogs

Using the output from the free ratios (model = 1) PAML runs, Fisher's exact test was used to test for asymmetry in the ratio of the estimated numbers of nonsynonymous and synonymous substitutions (Pegueroles et al., 2013). Nonsynonymous and synonymous substitution estimates were entered into the *fisher.test()* function in R with default parameters. For each pair of duplicates, a test between paralog 1 and paralog 2 was performed (**Figure 1**). If the paralogs were found to be evolving symmetrically, their combined numbers of substitutions were compared to those of the ancestral branch (**Figure 1**). If the paralogs were found to be evolving asymmetrically, each one was compared individually against the ancestral branch (**Figure 1**). The four cases in which there were more than two species-specific paralogs (*Soja max* and *Gossypium raimondii CLPP5*; *Musa acuminata* and *Vitis vinifera CLPR4*) were excluded from this analysis.

Data availability

Scripts, untrimmed and trimmed alignments, PAML output, and HyPhy output are provided for both *ACC* and Clp subunits at https://github.com/alissawilliams/Gene_duplication_ACCase_Clp.

Results:

Plastid-targeted ACCases evolve more rapidly than cytosol-targeted ACCases across angiosperms

Across the sampled clades (Geraniaceae, Caryophyllaceae, Brassicaceae, and Poaceae), nearly all plastid-targeted *ACC2* genes have higher d_N/d_S values than their cytosol-targeted *ACC1* counterparts (**Figure 2, Figure S1**). The single-partition model assigned all branches a d_N/d_S value of 0.1266, while the two-partition model assigned *ACC1* branches a value of 0.0883 and *ACC2* branches a value of 0.1936 ($\chi^2 = 466.84$, $p << 0.0001$). This pattern is true for both terminal and internal branches. The increase in in d_N/d_S ratios in *ACC2* branches is generally

driven by increases in d_N rather than reductions in d_S ($t = 4.48$, $p = 0.01$ for d_N; $t = 0.72$, $p = 0.5249$ for d_S; **Figure 2, Figure S2**), suggesting changes in selective pressure.

Using a branch-sites test in PAML (Yang, 2007), we did not find a significant signature of positive selection spanning the alignment ($\chi^2 = 0$, $p = 1$), although there were multiple individual sites found to be under positive selection (**Table S1**). Two HyPhy methods found limited, though significant, evidence for positive selection—the aBSREL run (Smith et al., 2015) detected one branch under positive selection ($p = 0.04$) and the BUSTED run (Murrell et al., 2015) assigned 0.12% of sites in foreground (*ACC2*) branches to the positive selection class relative to 0.05% of sites in background (*ACC1*) branches ($p = 0.0026$). The HyPhy RELAX method (Wertheim et al., 2015) found significant evidence for relaxed selection in the *ACC2* branches relative to the rest of the tree ($K = 0.09$, $p << 0.001$).

Characterizing ongoing duplication of nuclear-encoded Clp core subunit genes in angiosperms

Of the 23 angiosperm species in our dataset, 11 had one or more duplications of nuclear genes encoding Clp core subunits, and all eight of these genes were duplicated in at least one species (**Figure 3**). Most of these duplications were represented by two paralogs, but in four cases, we identified more than two paralogs for a particular subunit in a particular species. For *CLPP5*, *Soja max* and *Gossypium raimondii* have five and seven copies, respectively, and for *CLPR4*, both *Musa acuminata* and *Vitis vinifera* have four copies.

Soja max had duplications of the largest number of subunits (six of eight), followed by *Plantago maritima* and *Populus trichocarpa* with duplications of five subunits. Of the 11 species with duplications, *Eucalyptus grandis* and *Oenothera biennis* were the only species that had duplications of just one subunit. Across subunits, *CLPP5* had the highest number of paralogs (37 in 23 species) and *CLPR2* had the lowest (24 in 23 species).

In total, we identified 72 gene copies of Clp core subunits resulting from duplication events, including 40 catalytic subunits (*CLPP3-CLPP6*) (**Figure 3**). Of the 40 catalytic paralogs, we

found evidence of loss of one or more catalytic sites in multiple genes (**Table S2**). Across all 72 paralogs, we also found evidence of truncation of multiple different gene copies (including some with catalytic site loss) (**Table S2, Table S3**).

Recent paralogs of Clp core subunits tend to have higher rates of protein sequence evolution than their single-copy counterparts

Out of the eight nuclear-encoded Clp core subunit trees (**Figures S3-S10**), seven showed statistically significant differences between a model that allowed for different d_N/d_S rates in gene duplicates vs. single-copy genes (the three-partition model) and one that forces the same d_N/d_S rate on these two types of branches (the two-partition model) based on an uncorrected significance threshold of $p = 0.05$. (**Figure 4, Table 1**). In six of those cases, duplicated terminal branches had a higher d_N/d_S rate than non-duplicated terminal branches, while in the remaining case, the reverse was true. We separated internal branches from terminal branches to account for the fact that terminal branches will, on average, have higher d_N/d_S estimates than internal branches because selection has had more time to act on older deleterious mutations (Hasegawa et al., 1998; Ho et al., 2005). Further, terminal branches represent both interspecific divergence and intraspecific polymorphism, which is important because the latter inflates evolutionary rate calculations (Ho et al., 2005; Moilanen and Majamaa, 2003; Nielsen and Weinreich, 1999).

We also compared the evolutionary rates of paralogs to one another as well as to their common ancestor, again using an uncorrected significance threshold of $p = 0.05$ (**Table 2**). Of the 26 pairs of paralogs, 13 (50%) showed statistically significant rate asymmetry relative to each another. In 10 (77%) of those cases, only one paralog had a significantly different evolutionary rate than the common ancestor (and in all 10 of those cases, that paralog was evolving at a faster rate than the common ancestor). Of the 13 pairs with symmetric evolutionary rates, five (38%) were asymmetric relative to the common ancestor. In three of those cases, the combined paralog evolutionary rate was significantly faster than that of the ancestor.

Discussion:

Neofunctionalization and accelerated evolution of duplicated *ACC* genes in multiple clades of flowering plants

Independent duplications of *ACC* and subsequent retargeting events have been previously reported in multiple angiosperm clades (Babiychuk et al., 2011; Konishi and Sasaki, 1994; Park et al., 2017; Parker et al., 2014; Rockenbach et al., 2016; Schulte et al., 1997). The process of retargeting of a paralog is inherently a form of neofunctionalization because the newly retargeted protein functions in a different cellular compartment than it did ancestrally. A hallmark of neofunctionalization is evolutionary rate asymmetry between paralogs due to selection associated with gaining a new function (Hahn, 2009; Pegueroles et al., 2013; Zhang, 2003). We found that branches of our *ACC* tree representing paralogs targeted to the plastid had statistically significantly higher d_N/d_S values than branches representing paralogs targeted to the cytosol (**Figure 2, Figure S1**), consistent with the predictions under neofunctionalization. These results were based on a trimmed alignment lacking the target peptide, which we excluded because target peptides exhibit fast rates of evolution and reduced constraints on primary amino acid sequence (Bruce, 2001, 2000; Jarvis, 2008). Thus, our results show that *ACC* genes retargeted to the plastid are undergoing evolutionary rate increases unrelated to the target peptide, suggesting that other functional domains are also evolving rapidly.

Retargeting of the cytosolic, homomeric ACCase protein to the plastid is somewhat unexpected given that a heteromeric ACCase complex already exists in plastids. Whether the retargeted homomeric ACCases functionally replaces or coexists with the heteromeric version appears to vary across clades. In some angiosperm groups, the two complexes coexist, including in *Arabidopsis thaliana* and likely in other members of the Brassicaceae (Babiychuk et al., 2011; Rousseau-Gueutin et al., 2013). In other clades, the homomeric ACCase has replaced the heteromeric version, as was reported in the Poaceae (Konishi and Sasaki, 1994). The duplication found in *Silene noctiflora* and *Silene paradoxa* may also represent a replacement event given that both species lack at least one heteromeric ACCase gene each, where *S. noctiflora* lacks all of them (Rockenbach et al., 2016). In some cases, including *Monsonia emarginata* in the Geraniaceae, the plastid-encoded *accD* gene of the heteromeric complex has been transferred to the nuclear genome, again suggesting that the heteromeric version is still functional (Park et al.,

2017; Rousseau-Gueutin et al., 2013). These contrasting histories of replacement vs. coexistence may mean that duplicates in different clades are evolving under different selection regimes.

Variation in post-duplication fates could confound tests of selection conducted across the entire *ACC* tree. Using PAML and HyPhy (Murrell et al., 2015; Smith et al., 2015; Wertheim et al., 2015; Yang, 2007), we tested for positive selection and relaxed selection in *ACC2* genes relative to *ACC1* genes, both of which can contribute to increased rates of protein sequence evolution. The results were mixed; there is some evidence for relaxed selection across all *ACC2* branches as well as for positive selection in a small number of branches and sites (**Table S1**). Across the four families in our sample, the smallest ratio between mean *ACC2* d_N and mean *ACC1* d_N was found in the Poaceae (1.5 vs. 2.2-2.6 for the other three families). Since the heteromeric ACCase is completely absent in the Poaceae (Konishi and Sasaki, 1994), we would expect stronger purifying selection on the plastid homomeric ACCase in this clade compared to clades in which the two versions coexist. Thus, these results are consistent with the hypothesis that relaxed selection is contributing to rate accelerations and that there is greater relaxation of selection when homomeric and heteromeric ACCases functions redundantly in the plastid, though the evidence is still limited. The potential for positive selection on retargeted ACCases is intriguing given that these proteins are thought to perform the same function as the ancestral protein; it is possible that retargeted proteins are adapting to specific biochemical and/or osmotic conditions within the new destination. Increased evolutionary rates after subcellular retargeting have been previously noted, though we do not fully understand their underlying causes (Byun-McKay and Geeta, 2007; Marques et al., 2008).

Ongoing duplication of nuclear-encoded Clp core subunit genes is common in angiosperms

Across green plants, duplication of the plastid-encoded Clp core subunit gene *clpP1* has only been found in a handful of lineages (Williams et al., 2019). While other studies have identified recent duplications of nuclear-encoded Clp core subunit genes (Rockenbach et al., 2016; Williams et al., 2021), our work shows that duplications of these nuclear-encoded subunits are pervasive across angiosperms (**Figure 3**). Because we used a mix of transcriptomic and genomic data, we took into consideration the possibility of misidentifying transcript variants as paralogs

425 but our use of primary transcripts only and manual curation to remove hits that appeared to be
426 splice variants (see Materials and Methods) minimizes the risk of this type of error.
427
428 The prevalence of whole genome duplication in plants may partially explain the prevalence of
429 Clp core subunit duplication (Clark and Donoghue, 2018; De Bodt et al., 2005; del Pozo and
430 Ramirez-Parra, 2015; Flagel and Wendel, 2009; Panchy et al., 2016; Wendel et al., 2018). For
431 instance, *Soja max* is a partially diploidized tetraploid, meaning that this lineage underwent a
432 polyploidization event very recently and has only just started the subsequent process of genome
433 reduction (Shultz et al., 2006). *Soja max* had the largest number of duplicated subunits across our
434 sample, which is consistent with this history of whole genome duplication. Similarly, *Populus*
435 *trichopoda*, which tied for the second largest number of duplicated subunits, only recently
436 underwent genome reduction after whole genome duplication (Tuskan et al., 2006). In these
437 cases, we may simply be observing the short-term effects of polyploidization prior to returning to
438 a single copy of each of these genes.
439
440 **Subunit stoichiometry and subfunctionalization in the evolution of the plastid Clp complex**
441
442 Clp core subunit ratios have been studied in *Arabidopsis thaliana* (Olinares et al., 2011a). The
443 core consists of two rings—a ClpP1/ClpR1-4 ring with a 3:1:1:1:1 subunit ratio, respectively,
444 and a ClpP3-6 ring with a 1:2:3:1 subunit ratio, respectively (Olinares et al., 2011a). Despite the
445 high degree of structural similarity amongst the plastid Clp core subunits, core composition (i.e.
446 the number of each type of core subunit) does not appear to vary in *A. thaliana* (Olinares et al.,
447 2011a; Peltier et al., 2004). Due to the stability of subunit interactions in *A. thaliana*, Clp
448 complexes in other angiosperms are typically assumed to have the same ratios of core subunits,
449 but our results suggest that varied numbers of core subunit paralogs may lead to varied
450 stoichiometry across species. Additional work has shown that loss of catalytic activity in ClpP5
451 (present in three copies in *A. thaliana*) is lethal while loss of catalytic activity in ClpP3 (present
452 in one copy in *A. thaliana*) is tolerated, suggesting that core subunit composition may be flexible
453 given a threshold number of catalytic subunits (Liao et al., 2018).
454

In fact, core subunit composition has been dynamic throughout the evolutionary history of the green lineage. The Clp complex is widely conserved across bacteria; in most bacteria, including *E. coli*, the Clp core consists of 14 identical subunits (Nishimura and van Wijk, 2015; Yu and Houry, 2007). However, in cyanobacteria, several duplications have produced four core subunits—three catalytic ClpP subunits and one catalytically inactive ClpR subunit (Andersson et al., 2009; Stanne et al., 2007). In green lineage (Viridiplantae) plastids, which are descended from ancient cyanobacteria, gene duplication has continued to expand the number of genes incorporated into the Clp core to yield nine genes (*CLPP1,3-6*, *CLPR1-4*) (Nishimura and van Wijk, 2015). Interestingly, ClpR subunits are incorporated into the core despite their lack of catalytic activity; they are thought to play a structural role in the complex, including chaperone docking (Nishimura and van Wijk, 2015; Olinares et al., 2011b, 2011a; Sjögren and Clarke, 2011). In *A. thaliana*, the Clp chaperone is believed to bind only to the ClpP1/ClpR1-4 ring, whereas chaperone proteins bind to both rings of the Clp core in bacteria (Peltier et al., 2004; Yu and Houry, 2007). This ClpP/ClpR division of function (catalytic activity vs chaperone binding) is indicative of subfunctionalization. Further, though the plastid Clp core subunit genes share common ancestry and are structurally similar, knockouts of individual subunits tend to produce severe phenotypes, including lethality in several cases (Kim et al., 2009; Koussevitzky et al., 2007; Rudella et al., 2006).

Possible subfunctionalization in recent paralogs of Clp core subunits

Given that subfunctionalization has likely played a major role in plastid Clp complex evolution, we were particularly interested in whether we could identify subfunctionalization after more recent duplication events. Taken to an extreme, subfunctionalization would involve having one gene for each of the 14 core subunits, which would lead to further expansion of the typical nine core subunit genes. The total number of core subunits after including recent paralogs and the plastid-encoded ClpP1 was less than 14 in most species. *Musa acuminata*, *Plantago maritima*, and *Populus trichocarpa* had 14 each, *Soja max* had 17, and *Gossypium raimondii* had 15 (**Figure 3)**. The numbers larger than 14 were driven in both cases by multiple paralogs of *CLPP5*, with five and seven copies, respectively. ClpP5 has the largest number of subunits stoichiometrically among the eight nuclear-encoded subunits, so the fact that the two largest

numbers of paralogs were both found in *CLPP5* could potentially suggest that some species are moving toward a 1:1 relationship between genes and core subunits. However, this explanation is not supported by other evidence. For example, the other cases of >2 paralogs were found for *CLPR4*, which encodes a protein that is present in just a single copy in the core in *Arabidopsis*. Further, it is not clear that all of these paralogs are capable of producing functional proteins given truncations and loss of catalytic sites (**Table S2, Table S3**).

We tested for signatures of subfunctionalization by looking at evolutionary rate asymmetry. Under subfunctionalization, we would expect paralogs to evolve at symmetric rates relative to one another but asymmetrically relative to their common ancestor (Pegueroles et al., 2013). We found five of these cases in our dataset: *Plantago maritima CLPP3*, *Geranium maderense CLPP4, Medicago truncatula CLPP5, Populus trichocarpa CLPP5,* and *Soja max CLPR1* (**Table 2**). In cases of subfunctionalization, we would expect the paralogs to evolve more quickly than the common ancestor because of relaxed selection due to their more limited functional roles, which was only the case for the former three. In those three cases, the evidence is consistent with subfunctionalization, particularly given that all six involved paralogs are full length. Further, the *P. maritima CLPP3* paralogs share the same substitutions in all three catalytic sites, which indicates duplication after the loss of catalytic activity, and the *G. maderense CLPP4* and *M. truncatula CLPP5* paralogs all have fully retained catalytic triads (**Table S2**).

Possible pseudogenization or neofunctionalization in recent paralogs of Clp core subunits

Predictions about evolutionary rates under neofunctionalization are similar to predictions under the degeneration/gene loss model—one paralog will maintain the ancestral evolutionary rate while the other undergoes evolutionary rate acceleration (Hahn, 2009; Pegueroles et al., 2013; Zhang, 2003). Previous work in this complex has shown that even ClpP1 subunits demonstrating massive accelerations in evolutionary rate can still be functional, meaning that high evolutionary rates alone do not necessarily indicate pseudogenization (Barnard-Kubow et al., 2014; Williams et al., 2019, 2015). Other sequence features can help us differentiate between pseudogenization and neofunctionalization. For example, truncation of a sequence can be evidence that it is no longer producing a functional protein; additionally, for ClpP subunits, loss of catalytic sites may

also be an indication of degeneration/pseudogenization (though there may be exceptions, including the *P. maritima CLPP3* paralogs mentioned above). In our dataset, the paralogs of *Musa acuminata CLPP4* and *P. trichocarpa CLPP4* follow these patterns (**Table 2**). In each of these pairs, the paralogs are evolving asymmetrically, and the paralog with a faster rate of evolution is truncated and lacking all three catalytic sites, suggesting loss of function (**Table S2**). Another example of probable pseudogenization is found for the second copy of *M. acuminata CLPR1*. This paralog was annotated as two separate genes due to an internal stop codon, which would lead to a truncation in the resultant protein.

As for neofunctionalization, there are other cases in our dataset where paralogs evolving asymmetrically both have retained catalytic sites and are full length (for instance, *Geranium maderense CLPP5* and *Oenothera biennis CLPP5*). There are no known instances of retargeting of plastid Clp core subunits; thus, evolutionary drivers of neofunctionalization of duplicated subunits are unknown. It is possible that neofunctionalization in this complex could involve recruiting additional interacting proteins—the ClpT proteins, for instance, are involved in assembly of the core and are a recently evolutionary innovation specific to green plants (Colombo et al., 2014; Kim et al., 2015; Nishimura and van Wijk, 2015; Sjögren and Clarke, 2011). Additionally, ongoing work has identified potential new adapter proteins in the plastid Clp complex (Montandon et al., 2019; Nishimura et al., 2015). Another possibility is tissue-specific expression of paralogs, which has not been documented in the Clp complex but has been identified in mitochondrial complexes (Boss et al., 1997; Guerrero-Castillo et al., 2017; Sinkler et al., 2017).

Possible retention of Clp core paralogs under the gene dosage advantage hypothesis

We also have eight cases of symmetrically evolving paralogs that are also evolving symmetrically relative to the common ancestor (**Table 2**). Under our initial predictions, these would represent paralogs retained under the gene dosage advantage hypothesis (Hahn, 2009; Ohno, 1970; Pegueroles et al., 2013; Zhang, 2003). Of these eight paralog pairs, four are from *Soja max* (which had six total pairs of paralogs), and three are from *Populus trichocarpa* (which had five total pairs of paralogs). As described above, both of these species are in the process of

548 rediploidization after a recent whole genome duplication (Shultz et al., 2006; Tuskan et al.,
549 2006). It is possible that these results reflect the fact that the gene duplications happened so
550 recently that the paralogs have not had time to diverge. This possibility is further supported given
551 that the estimates of numbers of substitutions for many of these paralogs were so low that there
552 was virtually no power to detect significant asymmetry.
553
554 **Alternative hypotheses and future directions**
555
556 While we based our analyses on established expectations for evolutionary rates under different
557 post-duplication fates (gene dosage advantage, neofunctionalization, and subfunctionalization),
558 other work has challenged the universality of these predictions. He and Zhang (2005) outline the
559 subneofunctionalization model, in which gene duplicates undergo rapid subfunctionalization
560 followed by prolonged neofunctionalization. Asymmetric evolutionary rates are often assumed to
561 be the result of either neofunctionalization or degeneration, but subfunctionalization can also
562 occur in an asymmetric fashion (He and Zhang, 2005). This hypothesis could relate to some of
563 our results; cases of asymmetric evolutionary rates could be due to subfunctionalization rather
564 than neofunctionalization. Additionally, functional constraint can also exist under
565 neofunctionalization, leading to lower substitution rates and possibly symmetric rates of
566 evolution, meaning that symmetrically evolving paralogs could represent cases of
567 neofunctionalization rather than subfunctionalization or gene dosage advantage (He and Zhang,
568 2005).
569
570 Regardless, our results demonstrate that post-duplication evolutionary fates of paralogs vary
571 widely across clades, even when the same genes are involved. Duplications of the homomeric
572 ACCase complex gene (*ACC*) and subsequent retargeting of one copy to the plastid have been
573 previously reported (Babiychuk et al., 2011; Konishi and Sasaki, 1994; Park et al., 2017; Parker
574 et al., 2014; Rockenbach et al., 2016; Schulte et al., 1997). Our results show that the retargeted
575 duplicates almost universally have increased d_N/d_S rates (**Figure 2, Figure S1**). As for plastid
576 Clp core subunit duplications, duplication has clearly shaped this complex over the course of
577 Viridiplantae evolution. We provide evidence of all possible post-duplication routes of recent
578 paralogs amongst the different subunits and different species in our dataset. Overall, our results

579 are compelling evidence that subunit ratios and stoichiometry may be dynamic across
580 angiosperm lineages. Isolation of plastid Clp complexes and analyses of subunit composition
581 have been performed in a handful of species (Moreno et al., 2017; Olinares et al., 2011a;
582 Williams et al., 2019); future work could determine these compositions in other angiosperms,
583 including those that have undergone recent gene duplications. Our work demonstrates that gene
584 duplication has been and continues to be an important force in plastid evolution.
585

586 **Acknowledgements**
587

588 This work was supported by a National Science Foundation (NSF) grant (MCB-1733227),
589 graduate fellowships from NSF (DGE-1321845) and the National Institutes of Health (T32-
590 GM132057), and the Wolves to Rams undergraduate research program (NSF Grant Numbers
591 1930150 and 19300092, NIH Grant Number 1T34GM137861-01).
592

593 **References**
594

595 Andersson, F.I., Tryggvesson, A., Sharon, M., Diemand, A.V., Classen, M., Best, C., Schmidt,
596 R., Schelin, J., Stanne, T.M., Bukau, B., Robinson, C.V., Witt, S., Mogk, A., Clarke,
597 A.K., 2009. Structure and function of a novel type of ATP-dependent Clp protease. J.
598 Biol. Chem. 284, 13519–13532. https://doi.org/10.1074/jbc.M809588200
599 Apitz, J., Nishimura, K., Schmied, J., Wolf, A., Hedtke, B., Wijk, K.J. van, Grimm, B., 2016.
600 Posttranslational Control of ALA Synthesis Includes GluTR Degradation by Clp Protease
601 and Stabilization by GluTR-Binding Protein. Plant Physiology 170, 2040–2051.
602 https://doi.org/10.1104/pp.15.01945
603 Babiychuk, E., Vandepoele, K., Wissing, J., Garcia-Diaz, M., Rycke, R.D., Akbari, H., Joubès,
604 J., Beeckman, T., Jänsch, L., Frentzen, M., Montagu, M.C.E.V., Kushnir, S., 2011.
605 Plastid gene expression and plant development require a plastidic protein of the
606 mitochondrial transcription termination factor family. PNAS 108, 6674–6679.
607 https://doi.org/10.1073/pnas.1103442108
608 Barnard-Kubow, K.B., Sloan, D.B., Galloway, L.F., 2014. Correlation between sequence
609 divergence and polymorphism reveals similar evolutionary mechanisms acting across
610 multiple timescales in a rapidly evolving plastid genome. BMC Evol Biol 14.
611 https://doi.org/10.1186/s12862-014-0268-y
612 Boss, O., Samec, S., Paoloni-Giacobino, A., Rossier, C., Dulloo, A., Seydoux, J., Muzzin, P.,
613 Giacobino, J.P., 1997. Uncoupling protein-3: a new member of the mitochondrial carrier
614 family with tissue-specific expression. FEBS Lett 408, 39–42.
615 https://doi.org/10.1016/s0014-5793(97)00384-0

616 Bouchnak, I., van Wijk, K.J., 2021. Structure, Function and Substrates of Clp AAA+ protease
617 systems in cyanobacteria, plastids and apicoplasts; a comparative analysis. Journal of
618 Biological Chemistry 100338. https://doi.org/10.1016/j.jbc.2021.100338
619 Bruce, B.D., 2001. The paradox of plastid transit peptides: conservation of function despite
620 divergence in primary structure. Biochimica et Biophysica Acta (BBA) - Molecular Cell
621 Research 1541, 2–21. https://doi.org/10.1016/S0167-4889(01)00149-5
622 Bruce, B.D., 2000. Chloroplast transit peptides: structure, function and evolution. Trends in Cell
623 Biology 10, 440–447. https://doi.org/10.1016/S0962-8924(00)01833-X
624 Byun-McKay, S.A., Geeta, R., 2007. Protein subcellular relocalization: a new perspective on the
625 origin of novel genes. Trends in Ecology & Evolution 22, 338–344.
626 https://doi.org/10.1016/j.tree.2007.05.002
627 Camacho, C., Coulouris, G., Avagyan, V., Ma, N., Papadopoulos, J., Bealer, K., Madden, T.L.,
628 2009. BLAST+: architecture and applications. BMC Bioinformatics 10, 421.
629 https://doi.org/10.1186/1471-2105-10-421
630 Caroca, R., Howell, K.A., Malinova, I., Burgos, A., Tiller, N., Pellizzer, T., Annunziata, M.G.,
631 Hasse, C., Ruf, S., Karcher, D., Bock, R., 2021. Knock-down of the plastid-encoded
632 acetyl-CoA carboxylase gene uncovers functions in metabolism and development. Plant
633 Physiology. https://doi.org/10.1093/plphys/kiaa106
634 Castresana, J., 2000. Selection of Conserved Blocks from Multiple Alignments for Their Use in
635 Phylogenetic Analysis. Molecular Biology and Evolution 17, 540–552.
636 https://doi.org/10.1093/oxfordjournals.molbev.a026334
637 Clark, J.W., Donoghue, P.C.J., 2018. Whole-Genome Duplication and Plant Macroevolution.
638 Trends in Plant Science 23, 933–945. https://doi.org/10.1016/j.tplants.2018.07.006
639 Colombo, C.V., Ceccarelli, E.A., Rosano, G.L., 2014. Characterization of the accessory protein
640 ClpT1 from Arabidopsis thaliana: oligomerization status and interaction with Hsp100
641 chaperones. BMC Plant Biology 14, 228. https://doi.org/10.1186/s12870-014-0228-0
642 Conant, G.C., Wagner, A., 2003. Asymmetric Sequence Divergence of Duplicate Genes.
643 Genome Res. 13, 2052–2058. https://doi.org/10.1101/gr.1252603
644 Darriba, D., Taboada, G.L., Doallo, R., Posada, D., 2011. ProtTest 3: fast selection of best-fit
645 models of protein evolution. Bioinformatics 27, 1164–1165.
646 https://doi.org/10.1093/bioinformatics/btr088
647 De Bodt, S., Maere, S., Van de Peer, Y., 2005. Genome duplication and the origin of
648 angiosperms. Trends in Ecology & Evolution 20, 591–597.
649 https://doi.org/10.1016/j.tree.2005.07.008
650 del Pozo, J.C., Ramirez-Parra, E., 2015. Whole genome duplications in plants: an overview from
651 Arabidopsis. Journal of Experimental Botany 66, 6991–7003.
652 https://doi.org/10.1093/jxb/erv432
653 Dermitzakis, E.T., Clark, A.G., 2001. Differential selection after duplication in mammalian
654 developmental genes. Mol Biol Evol 18, 557–562.
655 https://doi.org/10.1093/oxfordjournals.molbev.a003835
656 Des Marais, D.L., Rausher, M.D., 2008. Escape from adaptive conflict after duplication in an
657 anthocyanin pathway gene. Nature 454, 762–765. https://doi.org/10.1038/nature07092
658 Erixon, P., Oxelman, B., 2008. Whole-Gene Positive Selection, Elevated Synonymous
659 Substitution Rates, Duplication, and Indel Evolution of the Chloroplast clpP1 Gene.
660 PLOS ONE 3, e1386. https://doi.org/10.1371/journal.pone.0001386

661 Flagel, L.E., Wendel, J.F., 2009. Gene duplication and evolutionary novelty in plants. New
662 Phytologist 183, 557–564. https://doi.org/10.1111/j.1469-8137.2009.02923.x
663 Force, A., Lynch, M., Pickett, F.B., Amores, A., Yan, Y., Postlethwait, J., 1999. Preservation of
664 Duplicate Genes by Complementary, Degenerative Mutations. Genetics 151, 1531–1545.
665 Freeling, M., Lyons, E., Pedersen, B., Alam, M., Ming, R., Lisch, D., 2008. Many or most genes
666 in Arabidopsis transposed after the origin of the order Brassicales. Genome Res 18,
667 1924–1937. https://doi.org/10.1101/gr.081026.108
668 Goodstein, D.M., Shu, S., Howson, R., Neupane, R., Hayes, R.D., Fazo, J., Mitros, T., Dirks, W.,
669 Hellsten, U., Putnam, N., Rokhsar, D.S., 2012. Phytozome: a comparative platform for
670 green plant genomics. Nucleic Acids Research 40, D1178–D1186.
671 https://doi.org/10.1093/nar/gkr944
672 Green, B.R., 2011. Chloroplast genomes of photosynthetic eukaryotes. The Plant Journal 66, 34–
673 44. https://doi.org/10.1111/j.1365-313X.2011.04541.x
674 Guerrero-Castillo, S., Cabrera-Orefice, A., Huynen, M.A., Arnold, S., 2017. Identification and
675 evolutionary analysis of tissue-specific isoforms of mitochondrial complex I subunit
676 NDUFV3. Biochim Biophys Acta Bioenerg 1858, 208–217.
677 https://doi.org/10.1016/j.bbabio.2016.12.004
678 Guindon, S., Dufayard, J.-F., Lefort, V., Anisimova, M., Hordijk, W., Gascuel, O., 2010. New
679 Algorithms and Methods to Estimate Maximum-Likelihood Phylogenies: Assessing the
680 Performance of PhyML 3.0. Syst Biol 59, 307–321.
681 https://doi.org/10.1093/sysbio/syq010
682 Hahn, M.W., 2009. Distinguishing among evolutionary models for the maintenance of gene
683 duplicates. J Hered 100, 605–617. https://doi.org/10.1093/jhered/esp047
684 Hasegawa, M., Cao, Y., Yang, Z., 1998. Preponderance of slightly deleterious polymorphism in
685 mitochondrial DNA: nonsynonymous/synonymous rate ratio is much higher within
686 species than between species. Mol Biol Evol 15, 1499–1505.
687 https://doi.org/10.1093/oxfordjournals.molbev.a025877
688 He, X., Zhang, J., 2005. Rapid Subfunctionalization Accompanied by Prolonged and Substantial
689 Neofunctionalization in Duplicate Gene Evolution. Genetics 169, 1157–1164.
690 https://doi.org/10.1534/genetics.104.037051
691 Ho, S.Y.W., Phillips, M.J., Cooper, A., Drummond, A.J., 2005. Time Dependency of Molecular
692 Rate Estimates and Systematic Overestimation of Recent Divergence Times. Molecular
693 Biology and Evolution 22, 1561–1568. https://doi.org/10.1093/molbev/msi145
694 Huang, Y., Kendall, T., Forsythe, E.S., Dorantes-Acosta, A., Li, S., Caballero-Pérez, J., Chen,
695 X., Arteaga-Vázquez, M., Beilstein, M.A., Mosher, R.A., 2015. Ancient Origin and
696 Recent Innovations of RNA Polymerase IV and V. Mol Biol Evol 32, 1788–1799.
697 https://doi.org/10.1093/molbev/msv060
698 Jansen, R.K., Cai, Z., Raubeson, L.A., Daniell, H., dePamphilis, C.W., Leebens-Mack, J.,
699 Müller, K.F., Guisinger-Bellian, M., Haberle, R.C., Hansen, A.K., Chumley, T.W., Lee,
700 S.-B., Peery, R., McNeal, J.R., Kuehl, J.V., Boore, J.L., 2007. Analysis of 81 genes from
701 64 plastid genomes resolves relationships in angiosperms and identifies genome-scale
702 evolutionary patterns. PNAS 104, 19369–19374.
703 https://doi.org/10.1073/pnas.0709121104
704 Jarvis, P., 2008. Targeting of nucleus-encoded proteins to chloroplasts in plants. New
705 Phytologist 179, 257–285. https://doi.org/10.1111/j.1469-8137.2008.02452.x

706 Katoh, K., Standley, D.M., 2013. MAFFT Multiple Sequence Alignment Software Version 7:
707 Improvements in Performance and Usability. Mol Biol Evol 30, 772–780.
708 https://doi.org/10.1093/molbev/mst010
709 Kim, J., Kimber, M.S., Nishimura, K., Friso, G., Schultz, L., Ponnala, L., Wijk, K.J. van, 2015.
710 Structures, Functions, and Interactions of ClpT1 and ClpT2 in the Clp Protease System of
711 Arabidopsis Chloroplasts. The Plant Cell 27, 1477–1496.
712 https://doi.org/10.1105/tpc.15.00106
713 Kim, J., Rudella, A., Rodriguez, V.R., Zybailov, B., Olinares, P.D.B., Wijk, K.J. van, 2009.
714 Subunits of the Plastid ClpPR Protease Complex Have Differential Contributions to
715 Embryogenesis, Plastid Biogenesis, and Plant Development in Arabidopsis. The Plant
716 Cell 21, 1669–1692. https://doi.org/10.1105/tpc.108.063784
717 Kondrashov, F.A., Rogozin, I.B., Wolf, Y.I., Koonin, E.V., 2002. Selection in the evolution of
718 gene duplications. Genome Biol 3, RESEARCH0008. https://doi.org/10.1186/gb-2002-3-
719 2-research0008
720 Konishi, T., Sasaki, Y., 1994. Compartmentalization of two forms of acetyl-CoA carboxylase in
721 plants and the origin of their tolerance toward herbicides. PNAS 91, 3598–3601.
722 https://doi.org/10.1073/pnas.91.9.3598
723 Konishi, T., Shinohara, K., Yamada, K., Sasaki, Y., 1996. Acetyl-CoA Carboxylase in Higher
724 Plants: Most Plants Other Than Gramineae Have Both the Prokaryotic and the Eukaryotic
725 Forms of This Enzyme. Plant and Cell Physiology 37, 117–122.
726 https://doi.org/10.1093/oxfordjournals.pcp.a028920
727 Kosakovsky Pond, S.L., Poon, A.F.Y., Velazquez, R., Weaver, S., Hepler, N.L., Murrell, B.,
728 Shank, S.D., Magalis, B.R., Bouvier, D., Nekrutenko, A., Wisotsky, S., Spielman, S.J.,
729 Frost, S.D.W., Muse, S.V., 2020. HyPhy 2.5—A Customizable Platform for Evolutionary
730 Hypothesis Testing Using Phylogenies. Molecular Biology and Evolution 37, 295–299.
731 https://doi.org/10.1093/molbev/msz197
732 Koussevitzky, S., Stanne, T.M., Peto, C.A., Giap, T., Sjögren, L.L.E., Zhao, Y., Clarke, A.K.,
733 Chory, J., 2007. An <Emphasis Type="Italic">Arabidopsis thaliana</Emphasis>
734 virescent mutant reveals a role for ClpR1 in plastid development. Plant Mol Biol 63, 85–
735 96. https://doi.org/10.1007/s11103-006-9074-2
736 Leebens-Mack, J.H., Barker, M.S., Carpenter, E.J., Deyholos, M.K., Gitzendanner, M.A.,
737 Graham, S.W., Grosse, I., Li, Z., Melkonian, M., Mirarab, S., Porsch, M., Quint, M.,
738 Rensing, S.A., Soltis, D.E., Soltis, P.S., Stevenson, D.W., Ullrich, K.K., Wickett, N.J.,
739 DeGironimo, L., Edger, P.P., Jordon-Thaden, I.E., Joya, S., Liu, T., Melkonian, B.,
740 Miles, N.W., Pokorny, L., Quigley, C., Thomas, P., Villarreal, J.C., Augustin, M.M.,
741 Barrett, M.D., Baucom, R.S., Beerling, D.J., Benstein, R.M., Biffin, E., Brockington,
742 S.F., Burge, D.O., Burris, J.N., Burris, K.P., Burtet-Sarramegna, V., Caicedo, A.L.,
743 Cannon, S.B., Çebi, Z., Chang, Y., Chater, C., Cheeseman, J.M., Chen, T., Clarke, N.D.,
744 Clayton, H., Covshoff, S., Crandall-Stotler, B.J., Cross, H., dePamphilis, C.W., Der, J.P.,
745 Determann, R., Dickson, R.C., Di Stilio, V.S., Ellis, S., Fast, E., Feja, N., Field, K.J.,
746 Filatov, D.A., Finnegan, P.M., Floyd, S.K., Fogliani, B., García, N., Gâteblé, G., Godden,
747 G.T., Goh, F. (Qi Y., Greiner, S., Harkess, A., Heaney, J.M., Helliwell, K.E., Heyduk, K.,
748 Hibberd, J.M., Hodel, R.G.J., Hollingsworth, P.M., Johnson, M.T.J., Jost, R., Joyce, B.,
749 Kapralov, M.V., Kazamia, E., Kellogg, E.A., Koch, M.A., Von Konrat, M., Könyves, K.,
750 Kutchan, T.M., Lam, V., Larsson, A., Leitch, A.R., Lentz, R., Li, F.-W., Lowe, A.J.,
751 Ludwig, M., Manos, P.S., Mavrodiev, E., McCormick, M.K., McKain, M., McLellan, T.,

McNeal, J.R., Miller, R.E., Nelson, M.N., Peng, Y., Ralph, P., Real, D., Riggins, C.W., Ruhsam, M., Sage, R.F., Sakai, A.K., Scascitella, M., Schilling, E.E., Schlösser, E.-M., Sederoff, H., Servick, S., Sessa, E.B., Shaw, A.J., Shaw, S.W., Sigel, E.M., Skema, C., Smith, A.G., Smithson, A., Stewart, C.N., Stinchcombe, J.R., Szövényi, P., Tate, J.A., Tiebel, H., Trapnell, D., Villegente, M., Wang, C.-N., Weller, S.G., Wenzel, M., Weststrand, S., Westwood, J.H., Whigham, D.F., Wu, S., Wulff, A.S., Yang, Y., Zhu, D., Zhuang, C., Zuidof, J., Chase, M.W., Pires, J.C., Rothfels, C.J., Yu, J., Chen, C., Chen, L., Cheng, S., Li, J., Li, R., Li, X., Lu, H., Ou, Y., Sun, X., Tan, X., Tang, J., Tian, Z., Wang, F., Wang, J., Wei, X., Xu, X., Yan, Z., Yang, F., Zhong, X., Zhou, F., Zhu, Y., Zhang, Y., Ayyampalayam, S., Barkman, T.J., Nguyen, N., Matasci, N., Nelson, D.R., Sayyari, E., Wafula, E.K., Walls, R.L., Warnow, T., An, H., Arrigo, N., Baniaga, A.E., Galuska, S., Jorgensen, S.A., Kidder, T.I., Kong, H., Lu-Irving, P., Marx, H.E., Qi, X., Reardon, C.R., Sutherland, B.L., Tiley, G.P., Welles, S.R., Yu, R., Zhan, S., Gramzow, L., Theißen, G., Wong, G.K.-S., One Thousand Plant Transcriptomes Initiative, 2019. One thousand plant transcriptomes and the phylogenomics of green plants. Nature 574, 679–685. https://doi.org/10.1038/s41586-019-1693-2

Liao, J.-Y.R., Friso, G., Kim, J., Wijk, K.J. van, 2018. Consequences of the loss of catalytic triads in chloroplast CLPPR protease core complexes in vivo. Plant Direct 2, e00086. https://doi.org/10.1002/pld3.86

Lynch, M., Conery, J.S., 2000. The Evolutionary Fate and Consequences of Duplicate Genes. Science 290, 1151–1155. https://doi.org/10.1126/science.290.5494.1151

Lynch, M., Force, A., 2000. The Probability of Duplicate Gene Preservation by Subfunctionalization. Genetics 154, 459–473.

Maere, S., Bodt, S.D., Raes, J., Casneuf, T., Montagu, M.V., Kuiper, M., Peer, Y.V. de, 2005. Modeling gene and genome duplications in eukaryotes. PNAS 102, 5454–5459. https://doi.org/10.1073/pnas.0501102102

Majeran, W., Wollman, F.-A., Vallon, O., 2000. Evidence for a Role of ClpP in the Degradation of the Chloroplast Cytochrome b6f Complex. The Plant Cell 12, 137–149. https://doi.org/10.1105/tpc.12.1.137

Marques, A.C., Vinckenbosch, N., Brawand, D., Kaessmann, H., 2008. Functional diversification of duplicate genes through subcellular adaptation of encoded proteins. Genome Biol 9, R54. https://doi.org/10.1186/gb-2008-9-3-r54

Moilanen, J.S., Majamaa, K., 2003. Phylogenetic network and physicochemical properties of nonsynonymous mutations in the protein-coding genes of human mitochondrial DNA. Mol Biol Evol 20, 1195–1210. https://doi.org/10.1093/molbev/msg121

Montandon, C., Friso, G., Liao, J.-Y.R., Choi, J., van Wijk, K.J., 2019. In Vivo Trapping of Proteins Interacting with the Chloroplast CLPC1 Chaperone: Potential Substrates and Adaptors. J. Proteome Res. 18, 2585–2600. https://doi.org/10.1021/acs.jproteome.9b00112

Moreno, J.C., Tiller, N., Diez, M., Karcher, D., Tillich, M., Schöttler, M.A., Bock, R., 2017. Generation and characterization of a collection of knock-down lines for the chloroplast Clp protease complex in tobacco. J Exp Bot 68, 2199–2218. https://doi.org/10.1093/jxb/erx066

Murrell, B., Weaver, S., Smith, M.D., Wertheim, J.O., Murrell, S., Aylward, A., Eren, K., Pollner, T., Martin, D.P., Smith, D.M., Scheffler, K., Kosakovsky Pond, S.L., 2015.

797 Gene-Wide Identification of Episodic Selection. Molecular Biology and Evolution 32,
798 1365–1371. https://doi.org/10.1093/molbev/msv035
799 Nielsen, R., Weinreich, D.M., 1999. The age of nonsynonymous and synonymous mutations in
800 animal mtDNA and implications for the mildly deleterious theory. Genetics 153, 497–
801 506.
802 Nishimura, K., Apitz, J., Friso, G., Kim, J., Ponnala, L., Grimm, B., van Wijk, K.J., 2015.
803 Discovery of a Unique Clp Component, ClpF, in Chloroplasts: A Proposed Binary ClpF-
804 ClpS1 Adaptor Complex Functions in Substrate Recognition and Delivery. Plant Cell 27,
805 2677–2691. https://doi.org/10.1105/tpc.15.00574
806 Nishimura, K., Kato, Y., Sakamoto, W., 2017. Essentials of Proteolytic Machineries in
807 Chloroplasts. Molecular Plant 10, 4–19. https://doi.org/10.1016/j.molp.2016.08.005
808 Nishimura, K., van Wijk, K.J., 2015. Organization, function and substrates of the essential Clp
809 protease system in plastids. Biochimica et Biophysica Acta (BBA) - Bioenergetics, SI:
810 Chloroplast Biogenesis 1847, 915–930. https://doi.org/10.1016/j.bbabio.2014.11.012
811 Ohno, S., 1970. Evolution by Gene Duplication. Springer Science & Business Media.
812 Olinares, P.D.B., Kim, J., Davis, J.I., van Wijk, K.J., 2011a. Subunit stoichiometry, evolution,
813 and functional implications of an asymmetric plant plastid ClpP/R protease complex in
814 Arabidopsis. Plant Cell 23, 2348–2361. https://doi.org/10.1105/tpc.111.086454
815 Olinares, P.D.B., Kim, J., van Wijk, K.J., 2011b. The Clp protease system; a central component
816 of the chloroplast protease network. Biochimica et Biophysica Acta (BBA) -
817 Bioenergetics, Regulation of Electron Transport in Chloroplasts 1807, 999–1011.
818 https://doi.org/10.1016/j.bbabio.2010.12.003
819 Panchin, A.Y., Gelfand, M.S., Ramensky, V.E., Artamonova, I.I., 2010. Asymmetric and non-
820 uniform evolution of recently duplicated human genes. Biol Direct 5, 54.
821 https://doi.org/10.1186/1745-6150-5-54
822 Panchy, N., Lehti-Shiu, M., Shiu, S.-H., 2016. Evolution of Gene Duplication in Plants. Plant
823 Physiology 171, 2294–2316. https://doi.org/10.1104/pp.16.00523
824 Park, S., Ruhlman, T.A., Weng, M.-L., Hajrah, N.H., Sabir, J.S.M., Jansen, R.K., 2017.
825 Contrasting Patterns of Nucleotide Substitution Rates Provide Insight into Dynamic
826 Evolution of Plastid and Mitochondrial Genomes of Geranium. Genome Biol Evol 9,
827 1766–1780. https://doi.org/10.1093/gbe/evx124
828 Parker, N., Wang, Y., Meinke, D., 2014. Natural Variation in Sensitivity to a Loss of Chloroplast
829 Translation in Arabidopsis. Plant Physiology 166, 2013–2027.
830 https://doi.org/10.1104/pp.114.249052
831 Paterson, A.H., Chapman, B.A., Kissinger, J.C., Bowers, J.E., Feltus, F.A., Estill, J.C., 2006.
832 Many gene and domain families have convergent fates following independent whole-
833 genome duplication events in Arabidopsis, Oryza, Saccharomyces and Tetraodon. Trends
834 Genet 22, 597–602. https://doi.org/10.1016/j.tig.2006.09.003
835 Pegueroles, C., Laurie, S., Albà, M.M., 2013. Accelerated Evolution after Gene Duplication: A
836 Time-Dependent Process Affecting Just One Copy. Molecular Biology and Evolution 30,
837 1830–1842. https://doi.org/10.1093/molbev/mst083
838 Peltier, J.-B., Ripoll, D.R., Friso, G., Rudella, A., Cai, Y., Ytterberg, J., Giacomelli, L., Pillardy,
839 J., Wijk, K.J. van, 2004. Clp Protease Complexes from Photosynthetic and Non-
840 photosynthetic Plastids and Mitochondria of Plants, Their Predicted Three-dimensional
841 Structures, and Functional Implications. J. Biol. Chem. 279, 4768–4781.
842 https://doi.org/10.1074/jbc.M309212200

Porankiewicz, J., Wang, J., Clarke, A.K., 1999. New insights into the ATP-dependent Clp protease: Escherichia coli and beyond. Molecular Microbiology 32, 449–458. https://doi.org/10.1046/j.1365-2958.1999.01357.x

Renny-Byfield, S., Wendel, J.F., 2014. Doubling down on genomes: polyploidy and crop plants. Am J Bot 101, 1711–1725. https://doi.org/10.3732/ajb.1400119

Rizzon, C., Ponger, L., Gaut, B.S., 2006. Striking Similarities in the Genomic Distribution of Tandemly Arrayed Genes in Arabidopsis and Rice. PLOS Computational Biology 2, e115. https://doi.org/10.1371/journal.pcbi.0020115

Rockenbach, K., Havird, J.C., Monroe, J.G., Triant, D.A., Taylor, D.R., Sloan, D.B., 2016. Positive Selection in Rapidly Evolving Plastid–Nuclear Enzyme Complexes. Genetics 204, 1507–1522. https://doi.org/10.1534/genetics.116.188268

Rousseau-Gueutin, M., Huang, X., Higginson, E., Ayliffe, M., Day, A., Timmis, J.N., 2013. Potential Functional Replacement of the Plastidic Acetyl-CoA Carboxylase Subunit (accD) Gene by Recent Transfers to the Nucleus in Some Angiosperm Lineages. Plant Physiology 161, 1918–1929. https://doi.org/10.1104/pp.113.214528

Rudella, A., Friso, G., Alonso, J.M., Ecker, J.R., Wijk, K.J. van, 2006. Downregulation of ClpR2 Leads to Reduced Accumulation of the ClpPRS Protease Complex and Defects in Chloroplast Biogenesis in Arabidopsis. The Plant Cell 18, 1704–1721. https://doi.org/10.1105/tpc.106.042861

Salie, M.J., Thelen, J.J., 2016. Regulation and structure of the heteromeric acetyl-CoA carboxylase. Biochimica et Biophysica Acta (BBA) - Molecular and Cell Biology of Lipids, Plant Lipid Biology 1861, 1207–1213. https://doi.org/10.1016/j.bbalip.2016.04.004

Sasaki, Y., Nagano, Y., 2004. Plant Acetyl-CoA Carboxylase: Structure, Biosynthesis, Regulation, and Gene Manipulation for Plant Breeding. Bioscience, Biotechnology, and Biochemistry 68, 1175–1184. https://doi.org/10.1271/bbb.68.1175

Schulte, W., Töpfer, R., Stracke, R., Schell, J., Martini, N., 1997. Multi-functional acetyl-CoA carboxylase from Brassica napus is encoded by a multi-gene family: Indication for plastidic localization of at least one isoform. PNAS 94, 3465–3470. https://doi.org/10.1073/pnas.94.7.3465

Shultz, J.L., Kurunam, D., Shopinski, K., Iqbal, M.J., Kazi, S., Zobrist, K., Bashir, R., Yaegashi, S., Lavu, N., Afzal, A.J., Yesudas, C.R., Kassem, M.A., Wu, C., Zhang, H.B., Town, C.D., Meksem, K., Lightfoot, D.A., 2006. The Soybean Genome Database (SoyGD): a browser for display of duplicated, polyploid, regions and sequence tagged sites on the integrated physical and genetic maps of Glycine max. Nucleic Acids Res 34, D758-765. https://doi.org/10.1093/nar/gkj050

Sikosek, T., Chan, H.S., Bornberg-Bauer, E., 2012. Escape from Adaptive Conflict follows from weak functional trade-offs and mutational robustness. Proc Natl Acad Sci U S A 109, 14888–14893. https://doi.org/10.1073/pnas.1115620109

Sinkler, C.A., Kalpage, H., Shay, J., Lee, I., Malek, M.H., Grossman, L.I., Hüttemann, M., 2017. Tissue- and Condition-Specific Isoforms of Mammalian Cytochrome c Oxidase Subunits: From Function to Human Disease [WWW Document]. Oxidative Medicine and Cellular Longevity. https://doi.org/10.1155/2017/1534056

Sjögren, L.L.E., Clarke, A.K., 2011. Assembly of the chloroplast ATP-dependent Clp protease in Arabidopsis is regulated by the ClpT accessory proteins. Plant Cell 23, 322–332. https://doi.org/10.1105/tpc.110.082321

889 Sjögren, L.L.E., Stanne, T.M., Zheng, B., Sutinen, S., Clarke, A.K., 2006. Structural and
890 Functional Insights into the Chloroplast ATP-Dependent Clp Protease in Arabidopsis.
891 The Plant Cell 18, 2635–2649. https://doi.org/10.1105/tpc.106.044594
892 Sloan, D.B., Triant, D.A., Forrester, N.J., Bergner, L.M., Wu, M., Taylor, D.R., 2014. A
893 recurring syndrome of accelerated plastid genome evolution in the angiosperm tribe
894 Sileneae (Caryophyllaceae). Molecular Phylogenetics and Evolution 72, 82–89.
895 https://doi.org/10.1016/j.ympev.2013.12.004
896 Smith, M.D., Wertheim, J.O., Weaver, S., Murrell, B., Scheffler, K., Kosakovsky Pond, S.L.,
897 2015. Less Is More: An Adaptive Branch-Site Random Effects Model for Efficient
898 Detection of Episodic Diversifying Selection. Molecular Biology and Evolution 32,
899 1342–1353. https://doi.org/10.1093/molbev/msv022
900 Soltis, D.E., Albert, V.A., Leebens-Mack, J., Bell, C.D., Paterson, A.H., Zheng, C., Sankoff, D.,
901 Depamphilis, C.W., Wall, P.K., Soltis, P.S., 2009. Polyploidy and angiosperm
902 diversification. Am J Bot 96, 336–348. https://doi.org/10.3732/ajb.0800079
903 Stamatakis, A., 2014. RAxML version 8: a tool for phylogenetic analysis and post-analysis of
904 large phylogenies. Bioinformatics 30, 1312–1313.
905 https://doi.org/10.1093/bioinformatics/btu033
906 Stanne, T.M., Pojidaeva, E., Andersson, F.I., Clarke, A.K., 2007. Distinctive Types of ATP-
907 dependent Clp Proteases in Cyanobacteria. J. Biol. Chem. 282, 14394–14402.
908 https://doi.org/10.1074/jbc.M700275200
909 Taylor, J.S., Raes, J., 2004. Duplication and Divergence: The Evolution of New Genes and Old
910 Ideas. Annual Review of Genetics 38, 615–643.
911 https://doi.org/10.1146/annurev.genet.38.072902.092831
912 The Angiosperm Phylogeny Group, Chase, M.W., Christenhusz, M.J.M., Fay, M.F., Byng, J.W.,
913 Judd, W.S., Soltis, D.E., Mabberley, D.J., Sennikov, A.N., Soltis, P.S., Stevens, P.F.,
914 2016. An update of the Angiosperm Phylogeny Group classification for the orders and
915 families of flowering plants: APG IV. Botanical Journal of the Linnean Society 181, 1–
916 20. https://doi.org/10.1111/boj.12385
917 Tuskan, G.A., Difazio, S., Jansson, S., Bohlmann, J., Grigoriev, I., Hellsten, U., Putnam, N.,
918 Ralph, S., Rombauts, S., Salamov, A., Schein, J., Sterck, L., Aerts, A., Bhalerao, R.R.,
919 Bhalerao, R.P., Blaudez, D., Boerjan, W., Brun, A., Brunner, A., Busov, V., Campbell,
920 M., Carlson, J., Chalot, M., Chapman, J., Chen, G.-L., Cooper, D., Coutinho, P.M.,
921 Couturier, J., Covert, S., Cronk, Q., Cunningham, R., Davis, J., Degroeve, S., Déjardin,
922 A., Depamphilis, C., Detter, J., Dirks, B., Dubchak, I., Duplessis, S., Ehlting, J., Ellis, B.,
923 Gendler, K., Goodstein, D., Gribskov, M., Grimwood, J., Groover, A., Gunter, L.,
924 Hamberger, B., Heinze, B., Helariutta, Y., Henrissat, B., Holligan, D., Holt, R., Huang,
925 W., Islam-Faridi, N., Jones, S., Jones-Rhoades, M., Jorgensen, R., Joshi, C., Kangasjärvi,
926 J., Karlsson, J., Kelleher, C., Kirkpatrick, R., Kirst, M., Kohler, A., Kalluri, U., Larimer,
927 F., Leebens-Mack, J., Leplé, J.-C., Locascio, P., Lou, Y., Lucas, S., Martin, F.,
928 Montanini, B., Napoli, C., Nelson, D.R., Nelson, C., Nieminen, K., Nilsson, O., Pereda,
929 V., Peter, G., Philippe, R., Pilate, G., Poliakov, A., Razumovskaya, J., Richardson, P.,
930 Rinaldi, C., Ritland, K., Rouzé, P., Ryaboy, D., Schmutz, J., Schrader, J., Segerman, B.,
931 Shin, H., Siddiqui, A., Sterky, F., Terry, A., Tsai, C.-J., Uberbacher, E., Unneberg, P.,
932 Vahala, J., Wall, K., Wessler, S., Yang, G., Yin, T., Douglas, C., Marra, M., Sandberg,
933 G., Van de Peer, Y., Rokhsar, D., 2006. The genome of black cottonwood, Populus

trichocarpa (Torr. & Gray). Science 313, 1596–1604. https://doi.org/10.1126/science.1128691

Van de Peer, Y., Taylor, J.S., Braasch, I., Meyer, A., 2001. The Ghost of Selection Past: Rates of Evolution and Functional Divergence of Anciently Duplicated Genes. J Mol Evol 53, 436–446. https://doi.org/10.1007/s002390010233

Wang, W., Zheng, H., Fan, C., Li, J., Shi, J., Cai, Z., Zhang, G., Liu, D., Zhang, J., Vang, S., Lu, Z., Wong, G.K.-S., Long, M., Wang, J., 2006. High Rate of Chimeric Gene Origination by Retroposition in Plant Genomes. The Plant Cell 18, 1791–1802. https://doi.org/10.1105/tpc.106.041905

Welsch, R., Zhou, X., Yuan, H., Álvarez, D., Sun, T., Schlossarek, D., Yang, Y., Shen, G., Zhang, H., Rodriguez-Concepcion, M., Thannhauser, T.W., Li, L., 2018. Clp Protease and OR Directly Control the Proteostasis of Phytoene Synthase, the Crucial Enzyme for Carotenoid Biosynthesis in Arabidopsis. Mol Plant 11, 149–162. https://doi.org/10.1016/j.molp.2017.11.003

Wendel, J.F., Lisch, D., Hu, G., Mason, A.S., 2018. The long and short of doubling down: polyploidy, epigenetics, and the temporal dynamics of genome fractionation. Curr Opin Genet Dev 49, 1–7. https://doi.org/10.1016/j.gde.2018.01.004

Wertheim, J.O., Murrell, B., Smith, M.D., Kosakovsky Pond, S.L., Scheffler, K., 2015. RELAX: Detecting Relaxed Selection in a Phylogenetic Framework. Molecular Biology and Evolution 32, 820–832. https://doi.org/10.1093/molbev/msu400

Wheeler, D.L., Church, D.M., Federhen, S., Lash, A.E., Madden, T.L., Pontius, J.U., Schuler, G.D., Schriml, L.M., Sequeira, E., Tatusova, T.A., Wagner, L., 2003. Database resources of the National Center for Biotechnology. Nucleic Acids Res 31, 28–33.

Wicke, S., Schneeweiss, G.M., dePamphilis, C.W., Müller, K.F., Quandt, D., 2011. The evolution of the plastid chromosome in land plants: gene content, gene order, gene function. Plant Mol Biol 76, 273–297. https://doi.org/10.1007/s11103-011-9762-4

Williams, A.M., Friso, G., Wijk, K.J. van, Sloan, D.B., 2019. Extreme variation in rates of evolution in the plastid Clp protease complex. The Plant Journal 98, 243–259. https://doi.org/10.1111/tpj.14208

Williams, A.M., Itgen, M.W., Broz, A.K., Carter, O.G., Sloan, D.B., 2021. Long-read transcriptome and other genomic resources for the angiosperm Silene noctiflora. G3 Genes|Genomes|Genetics. https://doi.org/10.1093/g3journal/jkab189

Williams, A.V., Boykin, L.M., Howell, K.A., Nevill, P.G., Small, I., 2015. The Complete Sequence of the Acacia ligulata Chloroplast Genome Reveals a Highly Divergent clpP1 Gene. PLOS ONE 10, e0125768. https://doi.org/10.1371/journal.pone.0125768

Yang, Z., 2007. PAML 4: Phylogenetic Analysis by Maximum Likelihood. Mol Biol Evol 24, 1586–1591. https://doi.org/10.1093/molbev/msm088

Yang, Z., Nielsen, R., 2002. Codon-Substitution Models for Detecting Molecular Adaptation at Individual Sites Along Specific Lineages. Molecular Biology and Evolution 19, 908–917. https://doi.org/10.1093/oxfordjournals.molbev.a004148

Yu, A.Y.H., Houry, W.A., 2007. ClpP: A distinctive family of cylindrical energy-dependent serine proteases. FEBS Letters 581, 3749–3757. https://doi.org/10.1016/j.febslet.2007.04.076

Zhang, J., 2003. Evolution by gene duplication: an update. Trends in Ecology & Evolution 18, 292–298. https://doi.org/10.1016/S0169-5347(03)00033-8

Zhang, P., Gu, Z., Li, W.-H., 2003. Different evolutionary patterns between young duplicate genes in the human genome. Genome Biology 4, R56. https://doi.org/10.1186/gb-2003-4-9-r56

Zhang, Y., Ma, J., Yang, B., Li, R., Zhu, W., Sun, L., Tian, J., Zhang, L., 2014. The complete chloroplast genome sequence of Taxus chinensis var. mairei (Taxaceae): loss of an inverted repeat region and comparative analysis with related species. Gene 540, 201–209. https://doi.org/10.1016/j.gene.2014.02.037

Table 1: Differences in evolutionary rates between duplicated and non-duplicated plastid Clp core subunits. Reported *p*-values are based on likelihood ratio tests for 2-partition vs. 3-partition PAML models (see Materials and Methods). Log-likelihood (lnL) values are reported for each model.

Subunit	**lnL 2-partition model**	**lnL 3-partition model**	***p*-value**	**Class with higher d_N/d_S**
CLPP3	-10058.01	-10047.93	7.12e-06	Duplicated
CLPP4	-9606.41	-9552.26	<1.00e-10	Duplicated
CLPP5	-8121.80	-8070.90	<1.00e-10	Duplicated
CLPP6	-7697.62	-7691.31	3.82e-04	Non-duplicated
CLPR1	-14534.75	-14517.85	6.07e-09	Duplicated
CLPR2	-12018.69	-12002.74	1.63e-08	Duplicated
CLPR3	-10556.37	-10556.05	0.42	n/a
CLPR4	-10395.60	-10337.35	<1.00e-10	Duplicated

Table 2: *p*-values for asymmetries between paralogs and between paralogs and their common ancestor.

Species	**Gene**	**Paralog 1 vs. paralog 2**	**Paralog 1 vs. ancestor**	**Paralog 2 vs. ancestor**	**Paralogs 1+2 vs. ancestor**
P. maritima	*CLPP3*	0.83			1.25e-04*
S. max	*CLPP3*	1			0.20
P. maritima	*CLPP4*	1.28e-07	1.07e-09*	0.71	
M. acuminata	*CLPP4*	0.04	0.15	2.12e-04*	
S. max	*CLPP4*	0.57			1
P. trichocarpa	*CLPP4*	3.31e-04	3.44e-12*	1.76e-13*	
G. maderense	*CLPP4*	0.08			1.72e-03*
M. truncatula	*CLPP5*	1			3.61e-05*
P. trichocarpa	*CLPP5*	1			0.04^
O. biennis	*CLPP5*	9.12e-3	0.10	5.37e-4*	
G. maderense	*CLPP5*	1.71e-04	0.42	6.23e-4*	
S. max	*CLPP6*	0.27			1
P. trichocarpa	*CLPP6*	0.46			1
G. raimondii	*CLPP6*	0.71			1
M. acuminata	*CLPR1*	2.20e-16	0.82	2.20e-16*	
S. max	*CLPR1*	0.47			0.05^
P. trichocarpa	*CLPR1*	0.77			0.42
V. vinifera	*CLPR1*	4.45e-3	0.17	1.38e-09*	
M. guttatus	*CLPR1*	0.05	0.59	4.70e-04*	
P. maritima	*CLPR1*	4.70e-05	0.53	2.54e-05*	
P. maritima	*CLPR2*	0.01	0.18	1.63e-06*	
S. max	*CLPR3*	1			0.55
P. trichocarpa	*CLPR3*	0.34			0.35
M. truncatula	*CLPR4*	2.29e-03	0.21	0.11	
E. grandis	*CLPR4*	2.51e-05	0.68	5.42e-11*	
P. maritima	*CLPR4*	9.73e-05	9.53e-04	4.17e-14*	

* denotes that paralog(s) has/have significantly higher evolutionary rate than ancestor branch
^ denotes that paralog(s) has/have significantly lower evolutionary rate than ancestor branch

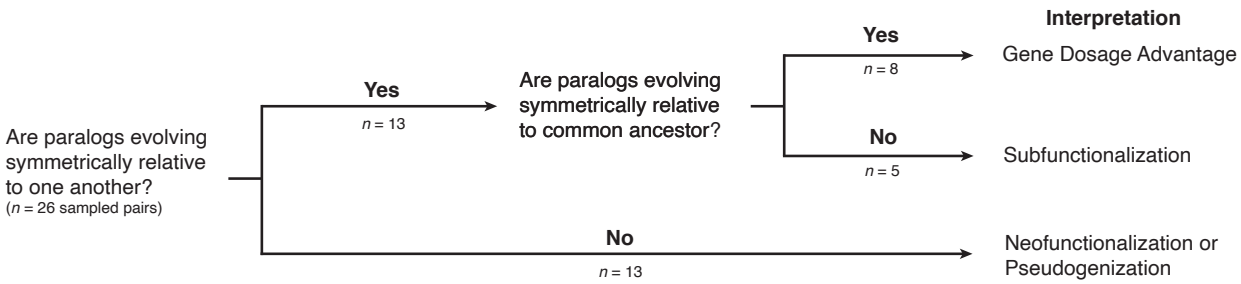

Figure 1: Expectations under different post-duplication models. For each pair of paralogs (n = 26), we first determined whether they were evolving symmetrically relative to one another using N and S estimates from PAML output. Paralogs evolving asymmetrically are predicted to represent neofunctionalization or pseudogenization events. For paralogs evolving symmetrically (n = 8), combined N and S values were compared to those of the immediate ancestor branch. Pairs evolving symmetrically relative to the common ancestor (n = 8) are predicted to represent gene dosage advantage while those evolving asymmetrically relative to the common ancestor (n = 5) are predicted to represent subfunctionalization.

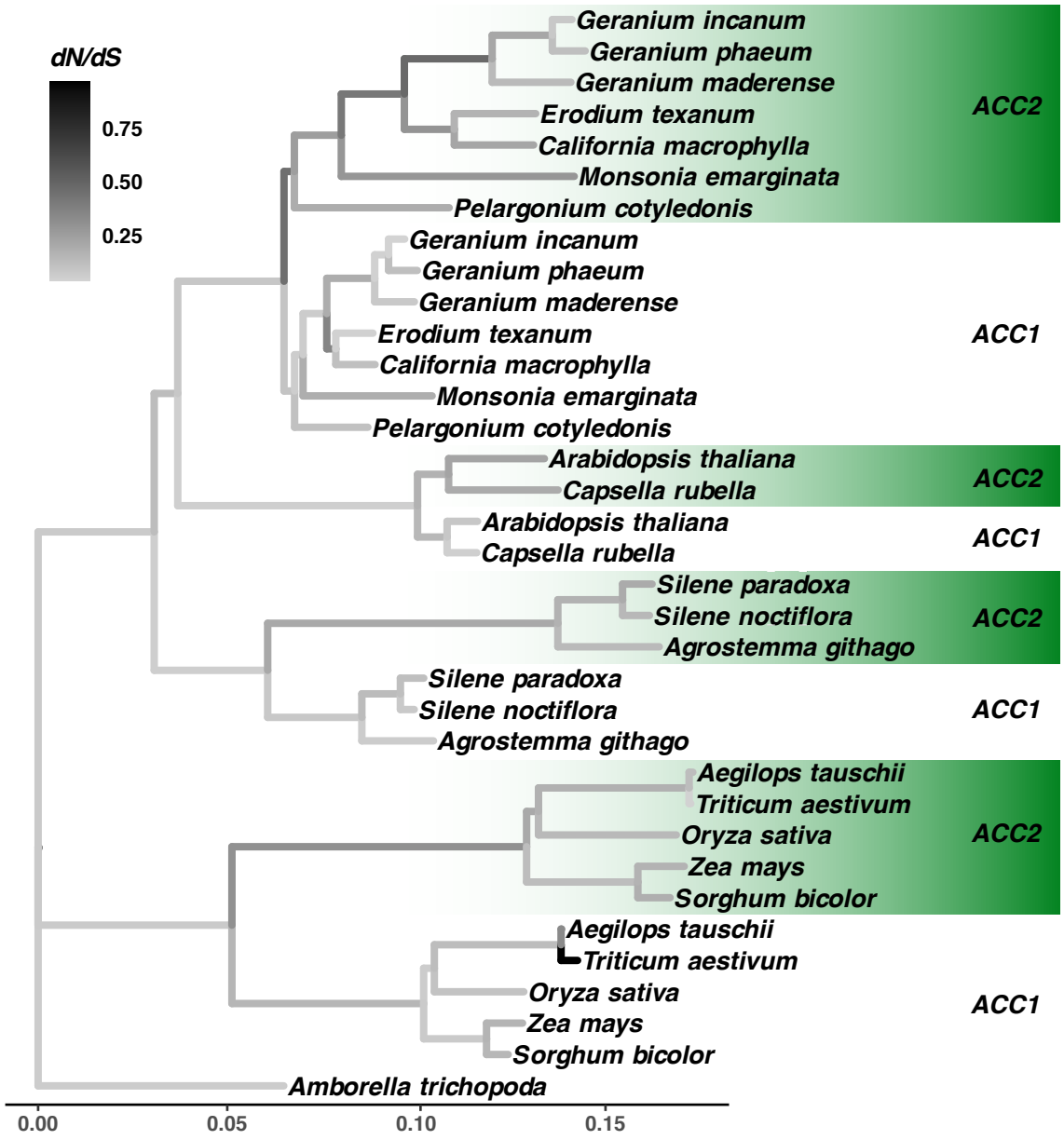

Figure 2: *ACC* genes across the Brassicaceae, Caryophyllaceae, Geraniaceae, and Poaceae, with the single copy of *ACC* in *Amborella trichopoda* as an outgroup. Branch lengths represent d_N values and branch colors represent d_N/d_S ratios.

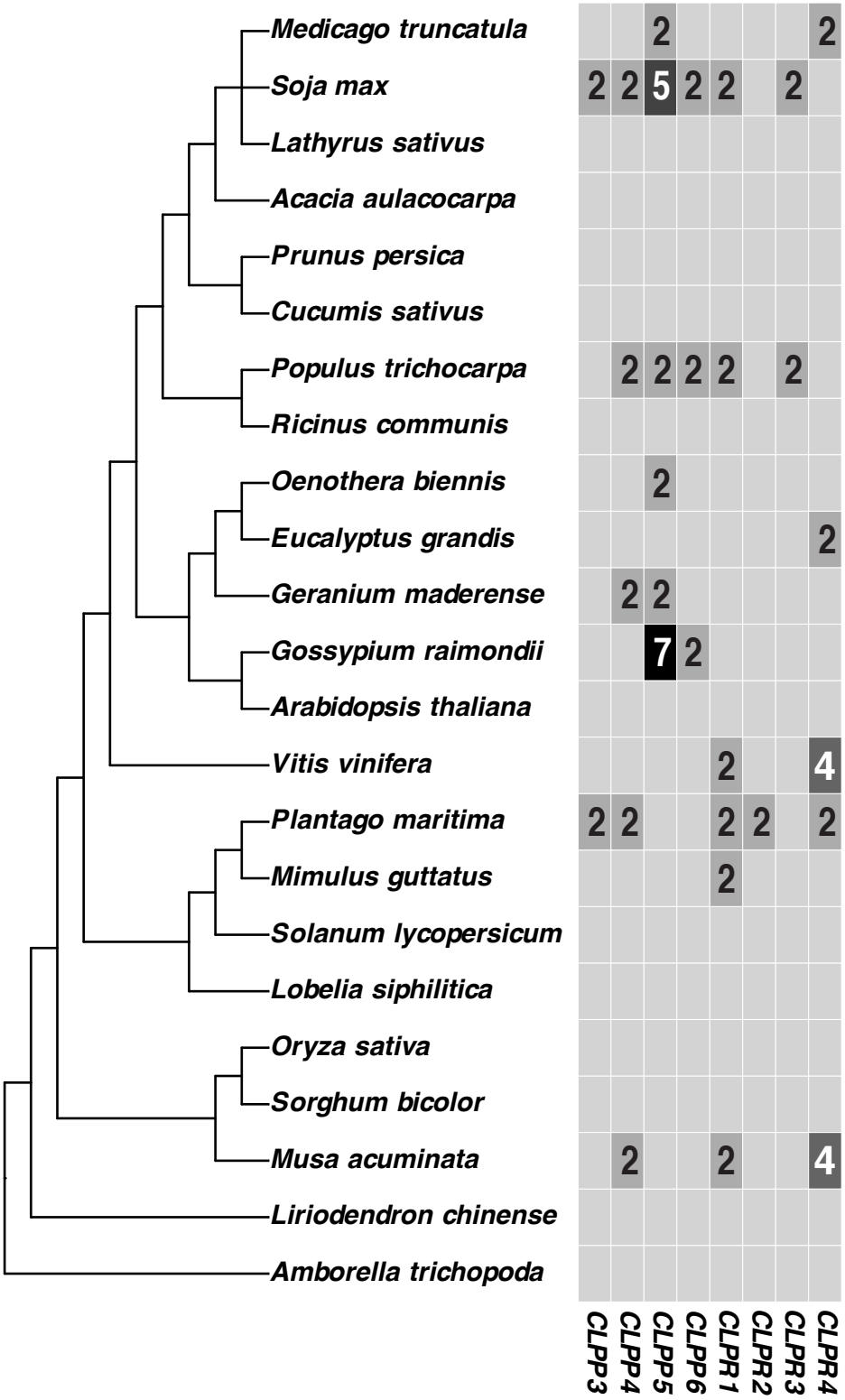

Figure 3: Copy numbers of the nuclear-encoded subunits of the plastid Clp core across angiosperms. Boxes without numbers indicate single-copy genes.

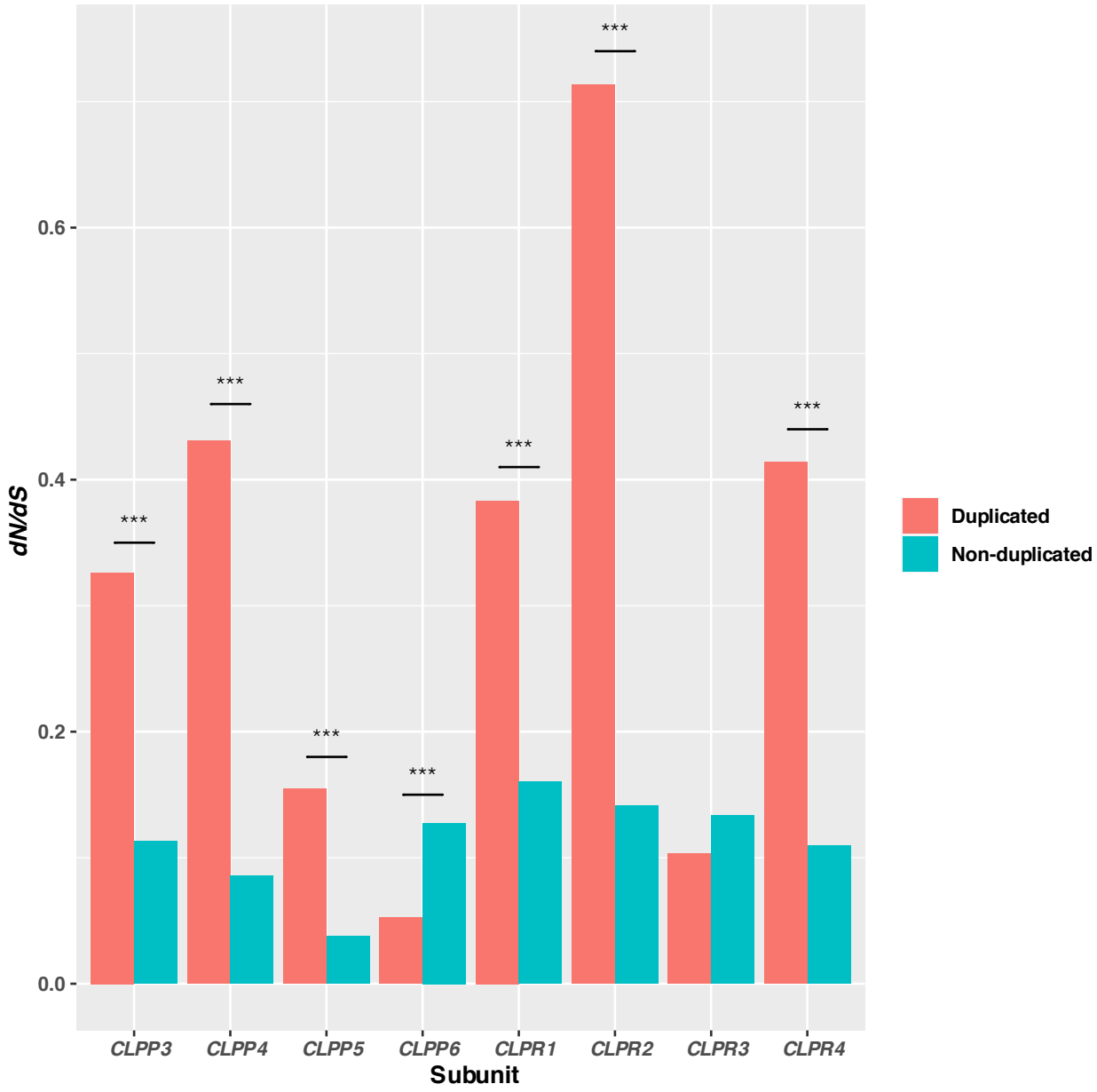

Figure 4: d_N/d_S ratios of duplicated and non-duplicated plastid Clp core subunits across angiosperms. The values were calculated using a PAML branch test with three groups, where each group was assigned its own d_N/d_S value: non-duplicated terminal branches, duplicated terminal branches (and in the cases of *CLPP5* and *CLPR4*, internal post-duplication branches), and internal branches. Significant differences ($p<<0.001$) are indicated with ***.

Table S1: Sites inferred to be under positive selection in *ACC2* branches based on a branch-sites test in PAML using the trimmed alignment for *ACC*.

Site	Amino acid	Probability
6	L	1.000
92	G	0.965
125	T	0.998
153	V	0.967
182	L	0.983
200	V	0.982
212	L	0.951
333	E	0.993
387	E	0.952
425	E	0.999
428	S	0.982
429	L	0.999
475	S	1.000
480	R	0.968
533	T	0.968
539	S	0.991
546	V	0.977
562	V	0.989
597	L	0.994
652	L	0.999
660	H	0.982
663	M	0.995
687	R	0.961
693	H	0.996
699	L	0.991
700	G	1.000
713	F	0.999
715	A	0.973
739	L	0.995
740	N	0.999
744	S	0.993
753	Q	0.980
766	D	0.967
769	N	0.990
776	K	0.986

794	L	0.967
797	G	0.996
837	R	0.997
849	S	0.996
859	Q	0.986
865	R	1.000
868	L	0.999
872	K	0.995
922	T	0.979
948	Q	0.985
973	T	0.984
981	T	0.999
982	P	0.999
985	K	0.998
989	N	0.999
991	R	0.997
1015	P	0.999
1027	R	0.999
1042	Q	0.991
1043	W	1.000
1044	H	1.000
1045	R	0.995
1048	L	0.978
1078	E	0.995
1085	W	0.980
1096	L	0.984
1108	T	0.999
1110	H	0.958
1147	M	0.990
1151	Q	0.994
1160	Q	0.998
1161	E	0.957
1168	K	1.000
1177	S	0.999
1197	R	0.998
1200	M	0.986
1212	Y	0.989
1243	A	0.995
1326	A	0.963

1342	I	0.981
1344	R	0.983
1507	S	0.952
1580	K	0.956
1602	R	0.971
1655	S	0.966
1735	L	1.000
1887	V	0.984
1898	A	0.999
1904	Q	0.985
1928	E	0.982
2021	P	0.958
2027	S	0.976
2063	E	1.000
2131	K	0.998
2135	E	0.962
2137	A	0.998
2164	G	0.965
2194	E	1.000
2230	P	1.000
2235	Q	0.992
2241	R	0.985
2245	G	0.976

Table S2: Loss of catalytic sites and truncation of nuclear-encoded plastid ClpP core subunits

Species	Protein	Serine	Histidine	Aspartate	Length
Eucalyptus grandis	ClpP3		Replaced with R		
Musa acuminata	ClpP3		Replaced with R		
Plantago maritima 1	ClpP3	Replaced with Y	Replaced with R	Replaced with N	
Plantago maritima 2	ClpP3	Replaced with Y	Replaced with R	Replaced with N	
Lathyrus sativus	ClpP4		Replaced with T		
Medicago truncatula	ClpP4		Replaced with A		
Musa acuminata 2	ClpP4	Gap	Replaced with R	Gap	Truncated
Plantago maritima 2	ClpP4			Gap	
Populus trichocarpa 2	ClpP4	Replaced with M	Gap	Gap	Truncated
Gossypium raimondii 3	ClpP5	Gap			
Gossypium raimondii 4	ClpP5				Truncated
Gossypium raimondii 5	ClpP5	Replaced with N			Truncated
Gossipium Raimondii 6	ClpP5	Replaced with N		Replaced with N	Truncated
Gossypium raimondii 7	ClpP5	Replaced with N		Replaced with F	
Plantago maritima	ClpP5	Gap	Gap	Gap	Truncated
Lathyrus sativus	ClpP6		Replaced with G		
Lobelia siphilitica	ClpP6	Replaced with N			
Medicago truncatula	ClpP6		Replaced with N		
Plantago maritima	ClpP6	Replaced with G	Replaced with E	Replaced with F	
Populus trichocarpa 2	ClpP6				Truncated

*Empty cell indicates presence of catalytic site or full length.

Table S3: Truncation of nuclear-encoded plastid ClpR core subunits

Truncated ClpR1 Subunits
Vitis vinifera 2
Populus trichocarpa 2
Musa acuminata 2 (internal stop codon)
Mimulus guttatus 2
Truncated ClpR2 Subunits
Plantago maritima 2
Truncated ClpR3 Subunits
Populus trichocarpa 1
Populus trichocarpa 2
Truncated ClpR4 Subunits
Eucalyptus grandis 2
Medicago truncatula 2
Vitis vinifera 2
Vitis vinifera 3
Vitis vinifera 4
Musa acuminata 3
Musa acuminata 4

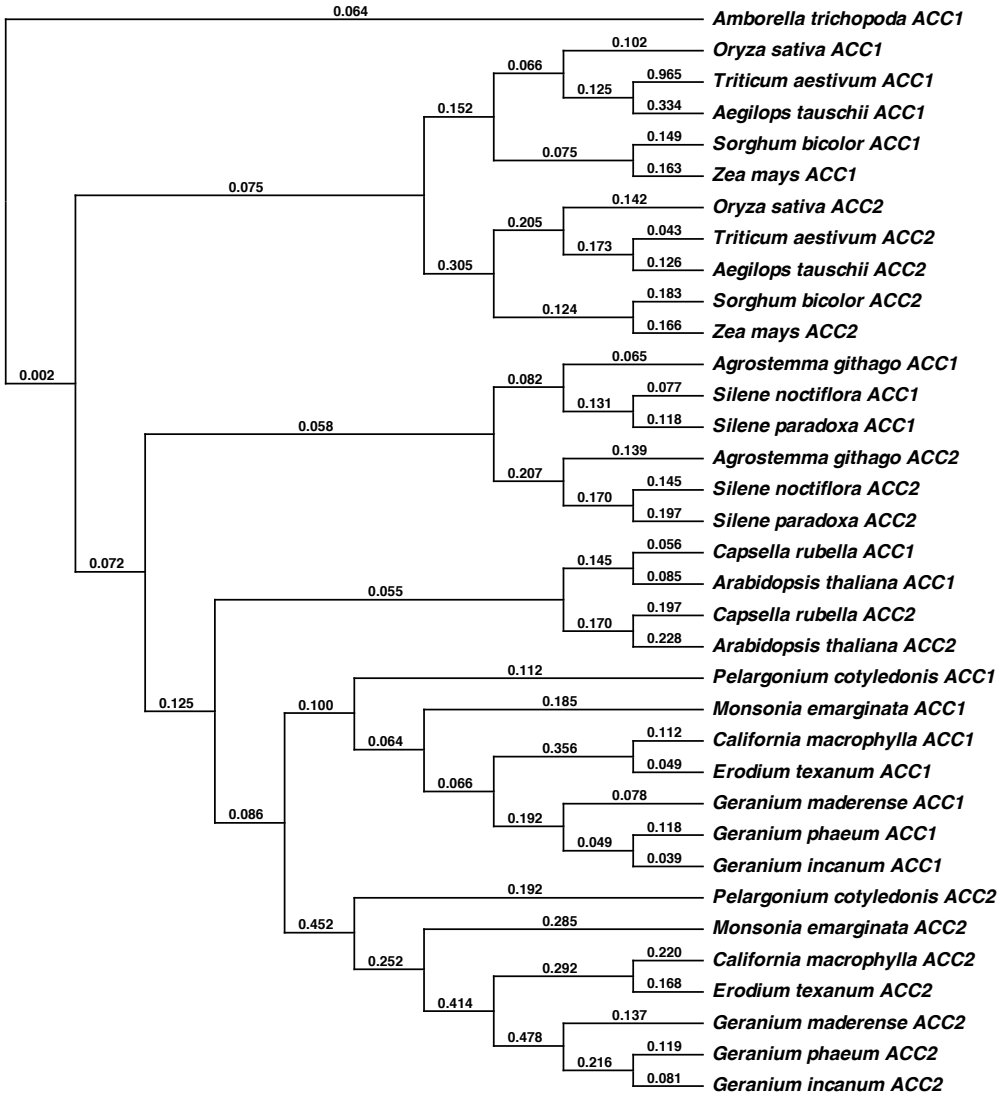

Figure S1. *ACC* tree. Branch labels are d_N/d_S values. *ACC1* represents cytosolic-targeted genes while *ACC2* represents plastid-targeted genes.

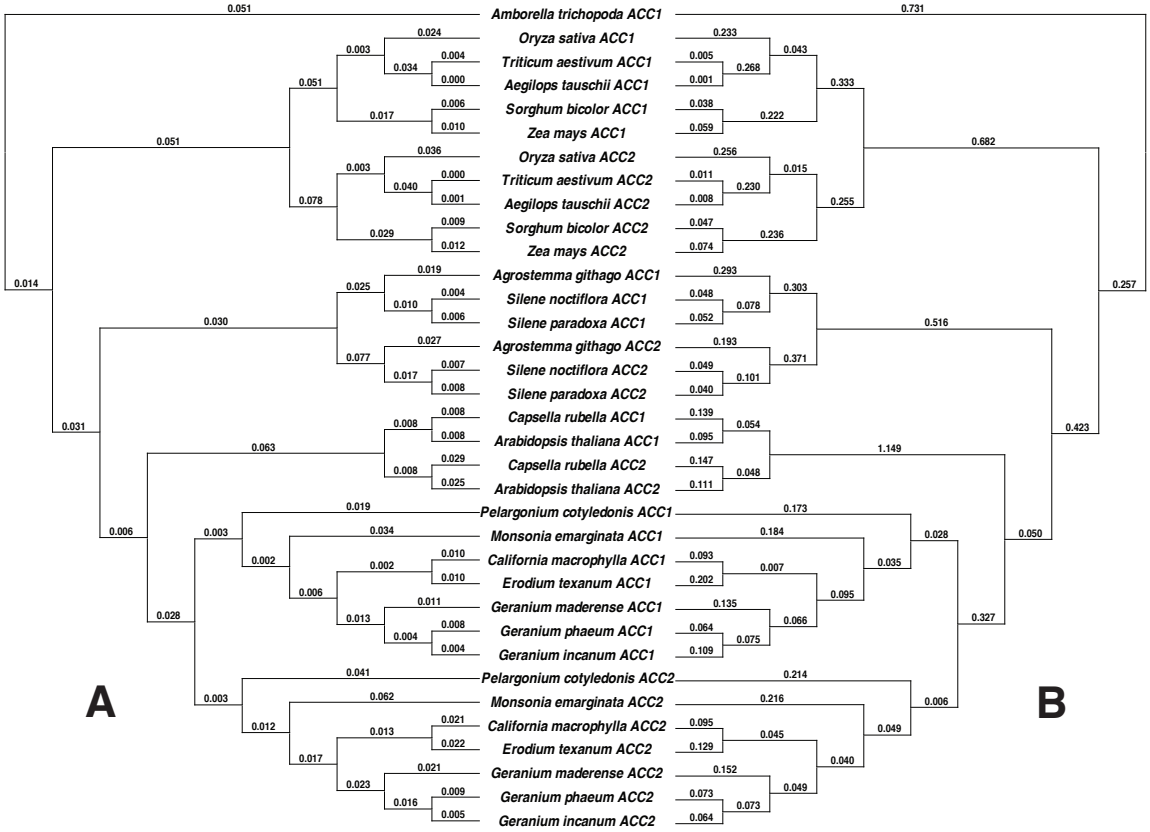

Figure S2. *ACC* tree. A) Branch labels are d_N values. B) Branch labels are d_S values.

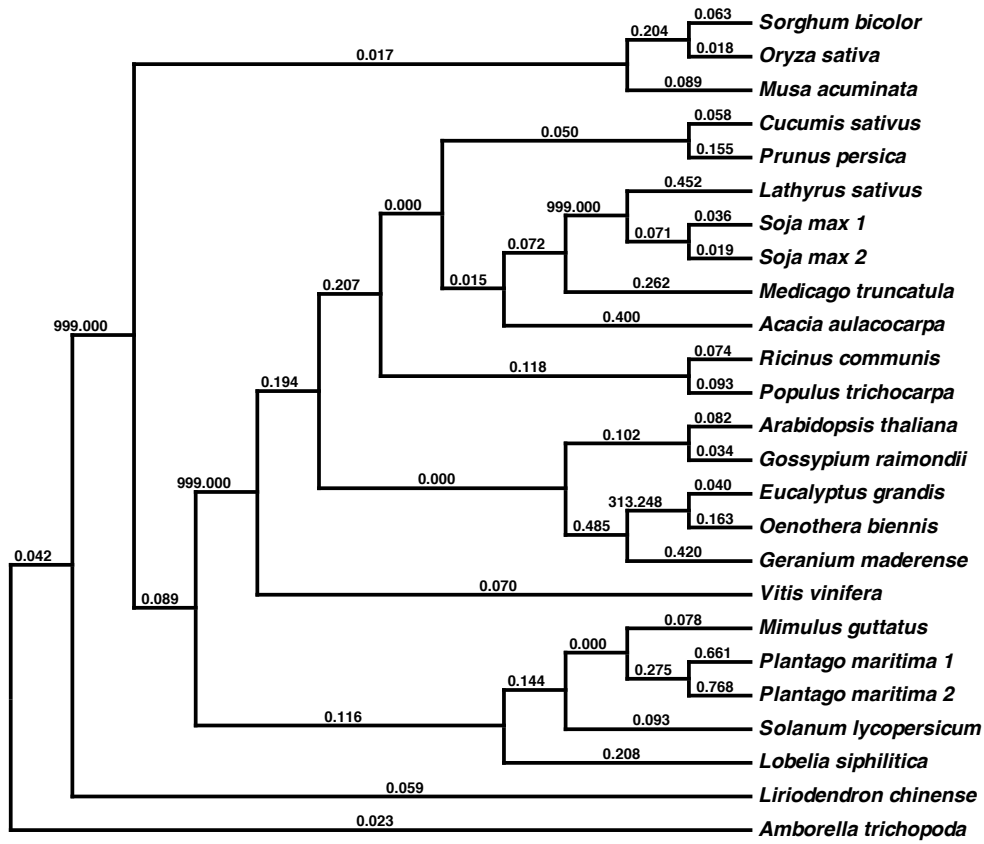

Figure S3. *CLPP3* tree. Branch labels are d_N/d_S values.

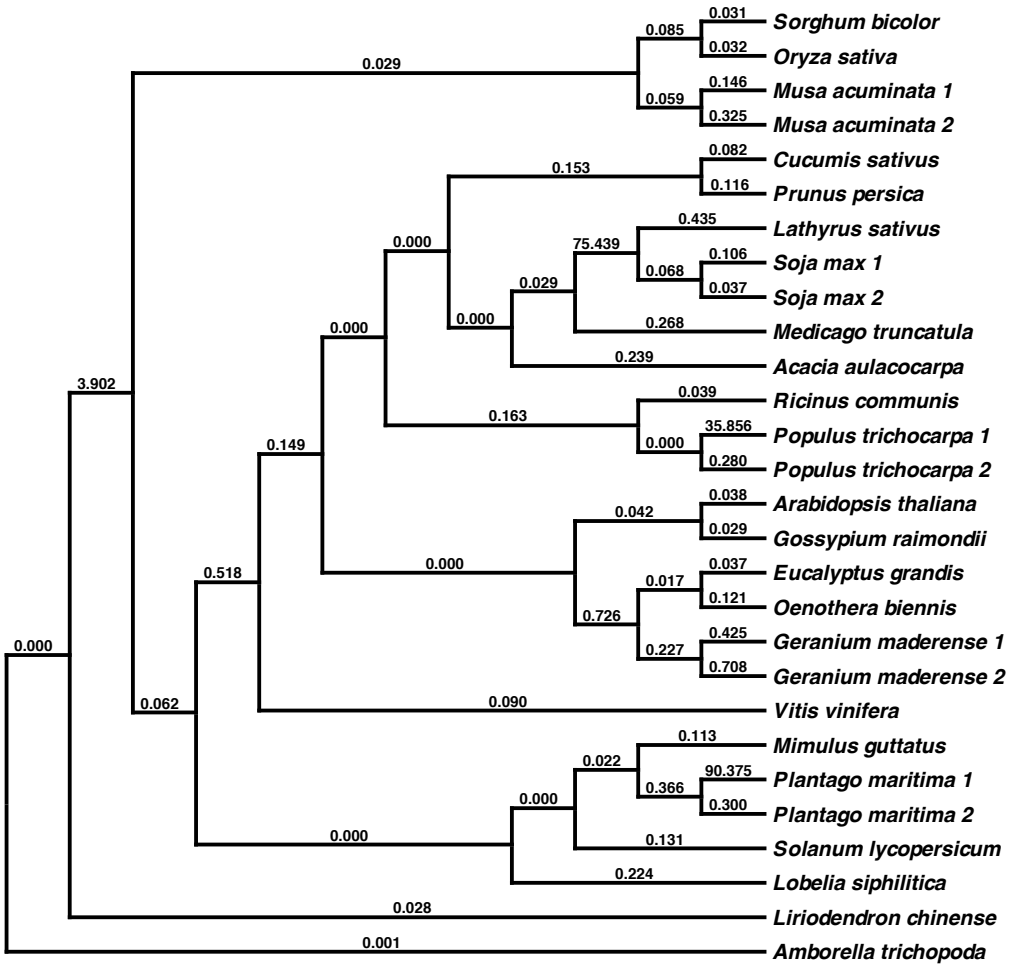

Figure S4. *CLPP4* tree. Branch labels are d_N/d_S values.

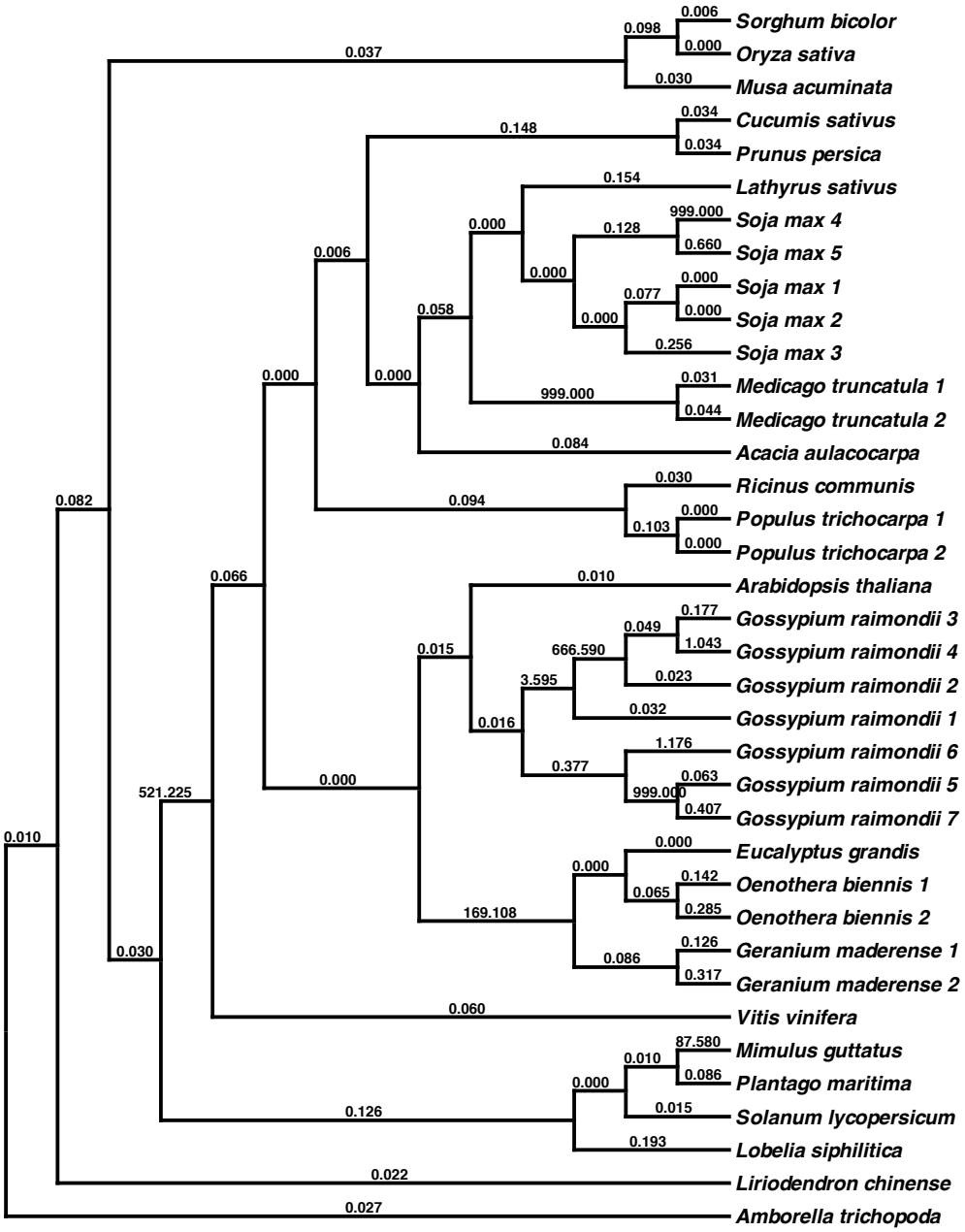

Figure S5. *CLPP5* tree. Branch labels are d_N/d_S values.

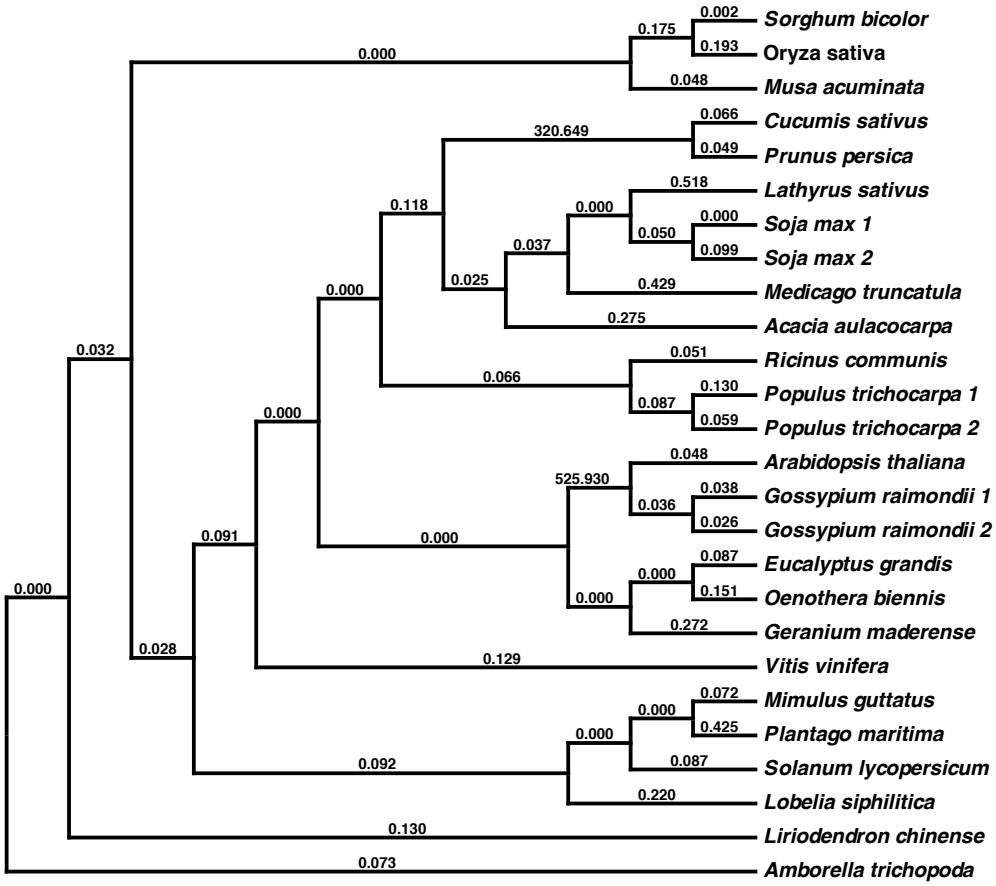

Figure S6. *CLPP6* tree. Branch labels are d_N/d_S values.

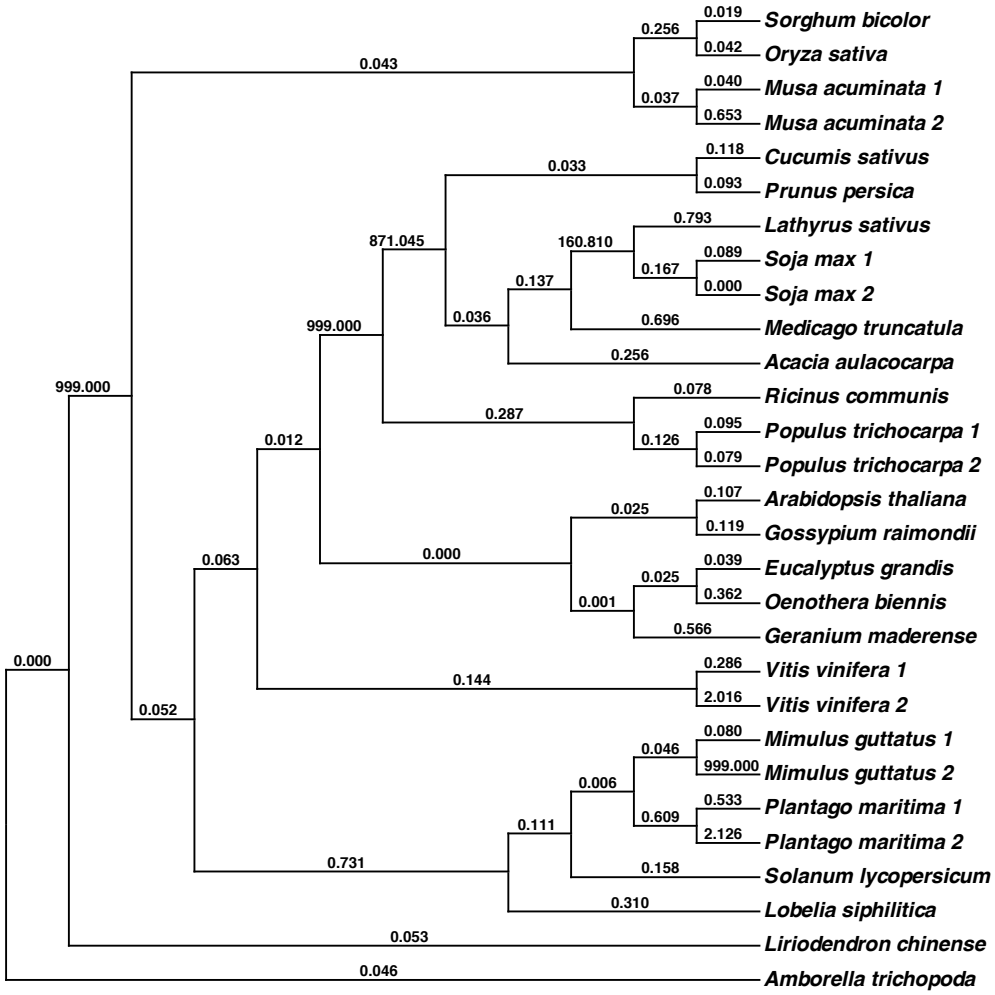

Figure S7. *CLPR1* tree. Branch labels are d_N/d_S values.

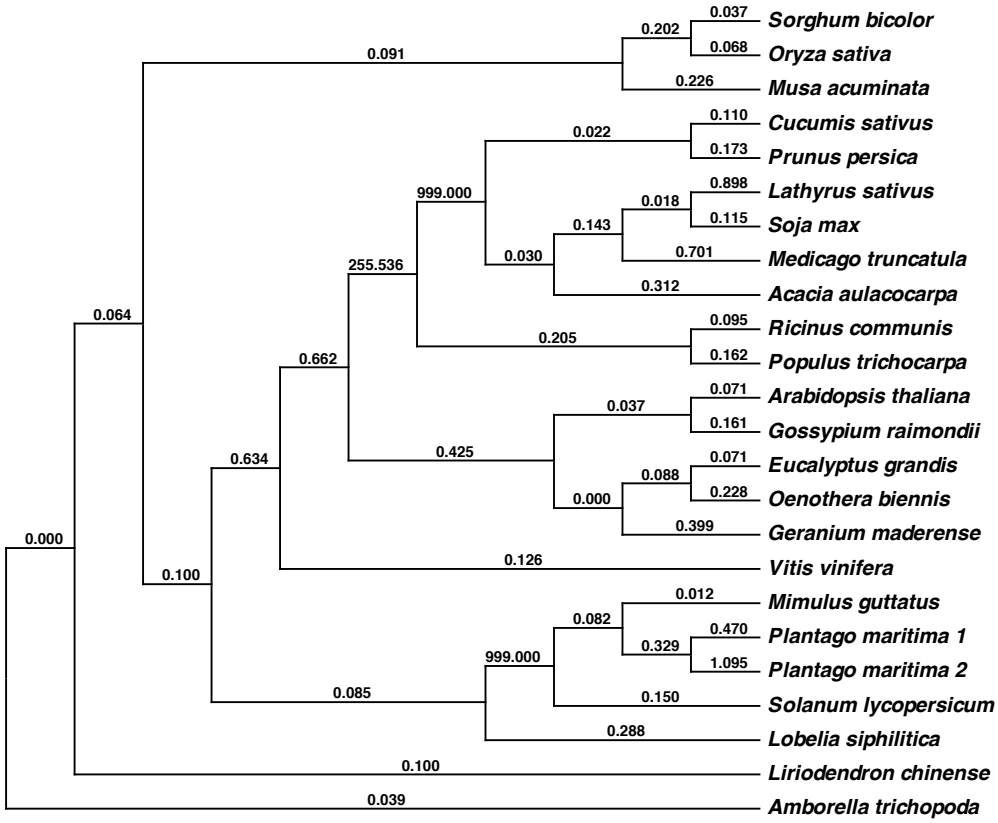

Figure S8. *CLPR2* tree. Branch labels are d_N/d_S values.

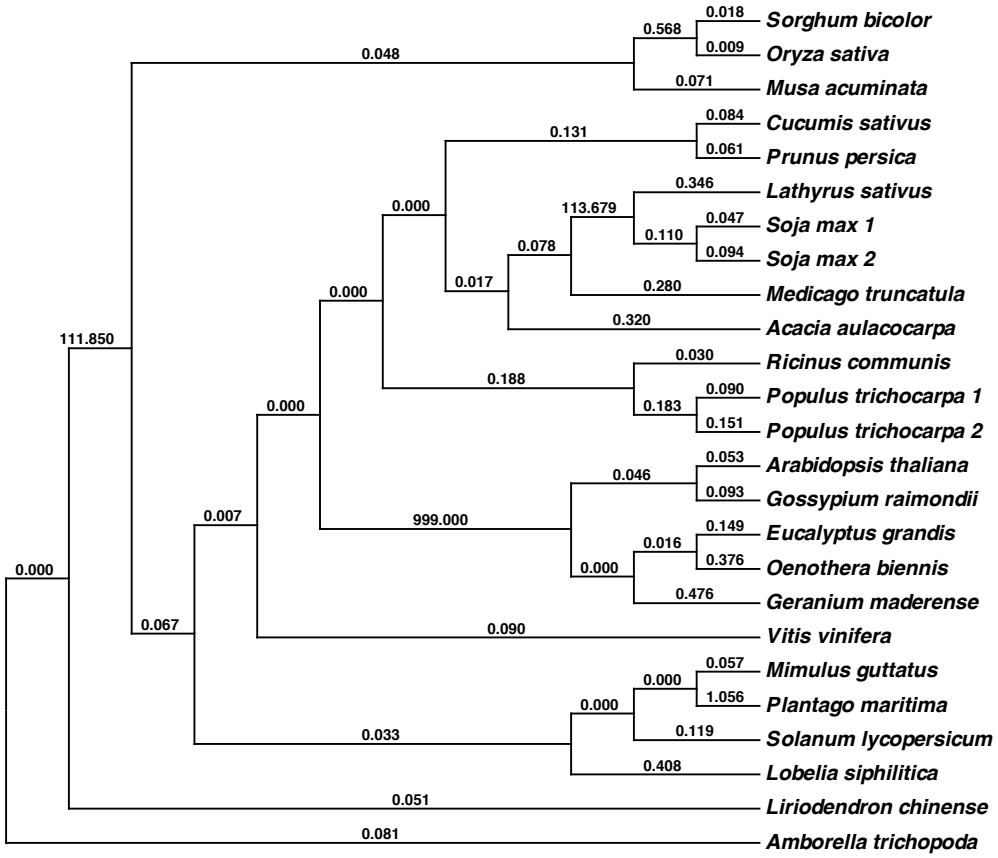

Figure S9. *CLPR3* tree. Branch labels are d_N/d_S values.

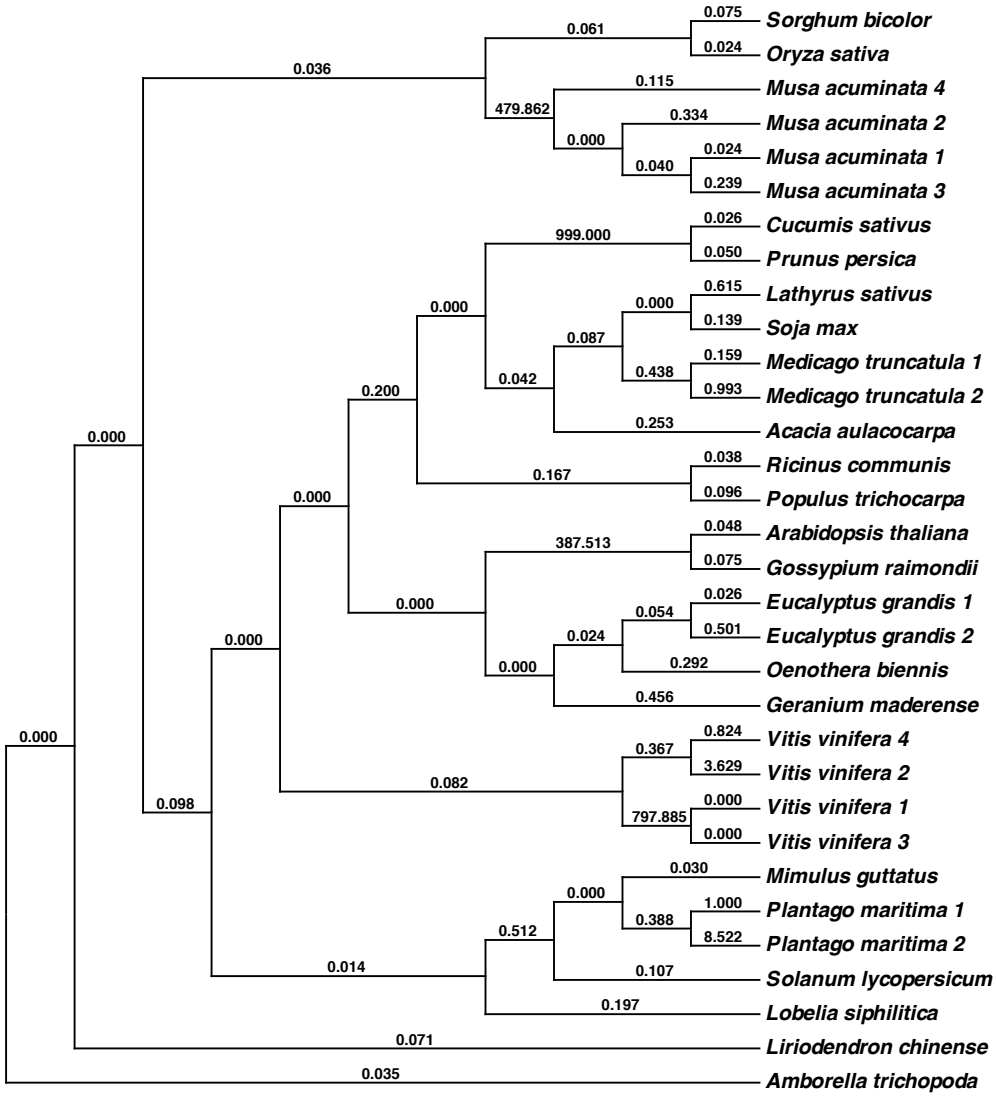

Figure S10. *CLPR4* tree. Branch labels are d_N/d_S values.